Experimental and computational aspects of molecular frustrated Lewis pairs for CO2 hydrogenation: en route for heterogeneous systems?

Riddhi Kumari Riddhi, Francesc Penas-Hidalgo, Hongmei Chen, Jérôme Canivet, Caroline Mellot-Draznieks, Albert Solé-Daura, Elsje Alessandra Quadrelli

Journal Name ARTICLE

Received 00th January 20xx,

Accepted 00th January 20xx

DOI: 10.1039/x0xx00000x

Experimental and computational aspects of molecular Frustrated Lewis Pairs for CO_2 hydrogenation: en route for heterogeneous systems?

Riddhi Kumari Riddhi,[a†] Francesc Penas-Hidalgo,[b†] Hongmei Chen,[b] Elsje Alessandra Quadrelli,[a] Jérôme Canivet,[a,*] Caroline Mellot-Draznieks,[b,*] Albert Solé-Daura[c,d,*]

Catalysis plays a crucial role in advancing sustainability. The unique reactivity of Frustrated Lewis Pairs (FLPs) is driving an ever-growing interest in the transition metal-free transformation of small molecules like CO_2 into valuable products. In this area, there is a recent growing incentive to heterogenize molecular FLPs into porous solids, merging the benefits of homogeneous and heterogeneous catalysis - high activity, selectivity, and recyclability. Despite the progress, challenges remain in preventing deactivation, poisoning, and simplifying catalyst-product separation. This review explores the expanding field of FLPs in catalysis, covering existing molecular FLPs for CO_2 hydrogenation and recent efforts to design heterogeneous porous systems from both experimental and theoretical perspectives. Section 2 discusses experimental examples of CO_2 hydrogenation by molecular FLPs, starting with stoichiometric reactions and advancing to catalytic ones. It then examines attempts to immobilize FLPs in porous matrices, including siliceous solids, metal-organic frameworks (MOFs), covalent organic frameworks, and disordered polymers, highlighting current limitations and challenges. Section 3 then reviews computational studies on the mechanistic details of CO_2 hydrogenation, focusing on H_2 splitting and hydride/proton transfer steps, summarizing efforts to establish structure-activity relationships. It also covers the computational aspects on grafting FLPs inside MOFs. Finally, section 4 summarizes the main design principles established so far, while addressing the complexities of translating computational approaches into experimental realm, particularly in heterogeneous systems. This section underscores the need to strengthen the dialogue between theoretical and experimental approaches in this field.

1. Introduction

Catalysis plays a key role in the manufacturing processes underlying our chemical industry. Still, there is an urgent need to reduce its environmental impact and to move towards a more sustainable society, which requires a careful reassessment of certain fundamental aspects. Many homogeneous and heterogeneous catalytic methods rely on transition metals as active sites. The use of such potentially scarce resources is coupled with limited recyclability and consequential resource waste in homogeneous systems, or with metal recovery using energy-intensive processes in heterogeneous systems.[1] Simultaneously, the direct conversion of small molecules into valuable synthetic intermediates, particularly employing CO_2 as a readily available and cost-effective C1 reservoir,[2] gains importance in increasing the sustainability of associated chemical processes.[3] Therefore, there is a persistent requirement to develop novel catalytic systems based on readily available, cost-effective elements with wide-ranging applicability, producing high-value compounds for environmentally friendly chemical production.

The advent of molecular Frustrated Lewis Pairs (FLPs), introduced by Stephan *et al.* in 2006,[4] showcases reactivity stemming from steric hindrance between Lewis acid (LA) and base (LB) partners, precluding the formation of the LA-LB adduct.[5–7] FLPs, often referred to as a "catalysis Holy Grail", have ushered in a new era of sustainable green chemistry. In particular, they allow the transition metal-free activation of small molecules, demonstrating significant potential in hydrogen activation and double bond reduction in fine chemicals, including CO_2 hydrogenation.[8–11]

While the field of homogeneous FLPs has gathered substantial knowledge in the past decade,[12,13] the transfer of FLPs' chemistry to heterogeneous catalysis is rather recent and garnering increasing interest. Besides addressing recyclability issues, the heterogenization of molecular FLPs allows the isolation of active sites within a controlled chemical environment, while preventing undesired interactions and catalyst deactivation. This isolation alters substrate activation interactions on the heterogeneous catalyst, leading to unprecedented reactivities explicable through molecular chemistry mechanisms. The development of heterogeneous FLPs is currently challenging and mainly limited to doped/defective oxide and metal surfaces.[14,15]

Incentives for discovering heterogeneous FLPs encompass aspects ranging from molecular-scale control over the distance between FLP's partners, influencing reactivity, to their recyclability, shaping, and scale-up production. Quantum mechanical calculations serve as a powerful tool for the *in silico* design of molecular architectures, having matured in molecular catalysis for predicting efficient systems, remarkably for asymmetric synthesis.[16–18] However, computational methodologies are at an earlier stage concerning heterogeneous catalysis.[19–22]

In addition to the perspectives on FLPs' chemistry by Stephan et al.,[14,23] recent reviews in the last five years have covered distinct advancements in FLPs' chemistry by considering either the realm of homogeneous catalysis[24–26] or strategies for their heterogenization into solid materials.[15,27,28] A recent review has been published on the

[a.] *IRCELYON, UMR 5256, Université LYON 1, 2 avenue Albert Einstein, 69626 Villeurbanne Cedex*
[b.] *Laboratoire de Chimie des Processus Biologiques, CNRS UMR 8229, Collège de France, PSL Research University, Sorbonne Université, 75231 Paris Cedex 05, France*
[c.] *Department de Química Física i Inorgànica, Universitat Rovira i Virgili, Marcel·lí Domingo 1, Tarragona 43007, Spain*
[d.] *Institute of Chemical Research of Catalonia (ICIQ-CERCA), The Barcelona Institute of Science and Technology, Avgda. Països Catalans, 16, 43007 Tarragona, Spain.*
† These authors contributed equally to this work.

specific area of the computational chemistry of FLPs, focusing exclusively on molecular FLPs.[29] Therefore, there remains a critical need for a comprehensive analysis of the recent progress and existing challenges in the discovery of FLP-based catalytic systems for CO_2 hydrogenation, encompassing both molecular and solid-state FLPs and integrating recent experimental and theoretical facets.

This review delves into fifteen years of FLPs chemistry development, exploring the chemistry of FLPs based on main group elements from experimental discovery to computational mechanistic dissection. The discussion encompasses the recent experimental advances of FLPs in catalytic processes, tools developed for their heterogenization, and key aspects of structure-activity relationships for CO_2 hydrogenation as determined *in silico*.

2. Experimentally reported FLPs for CO_2 hydrogenation

Since the pioneering report by Stephan *et al.* in 2006 with H_2 splitting by a transition metal-free P/B containing molecule,[4] this field exhibits an ever-expanding range of molecular LB (B, C, N, O, S, Se and Te) and LA (B, Al, Ga, In, C, Si, Sn, N and P) partners in intra- or inter-molecular fashions.[9,30] They demonstrated their large potential for the activation of H_2 and the subsequent reduction of double bonds in fine chemicals,[8,25] including CO_2 hydrogenation.[31–33] We will first summarize here the main experimental findings on FLP-mediated CO_2 hydrogenation using molecular H_2 (Table 1).

2.1. Molecular FLPs reported for non-catalytic and catalytic CO_2 reduction.

In this section, we aim to discuss the development of molecular FLPs and the study of their reactivity in biphasic gas-liquid systems from CO_2 activation to CO_2 hydrogenation, leading to unique catalytic systems. Here, FLPs are classified as either structurally intramolecular, i.e. the Lewis base (LB) and Lewis acid (LA) are part of the same molecule, or intermolecular, i.e. the LB and LA partners belong to two independent molecules.

2.1.1. Inter- and intramolecular FLPs based on BCF as Lewis acid

Tris(pentafluorophenyl)borane (BCF, $B(C_6F_5)_3$) is a widely used super Lewis acid which was first synthesised in the 1960s by Massey and coworkers[34,35] and used as an activator or cocatalyst for alkenes polymerization reactions.[36–38]

In 2009, Mömming, Stephan and coworkers described for the first time a novel approach for the metal-free binding of CO_2 by FLPs based on the combination of BCF and phosphine.[39] They demonstrated that the tBu$_3$P/B(C$_6$F$_5$)$_3$ FLP pair dissolved in bromobenzene can react with CO_2 under ambient pressure at room temperature to yield a white solid product tBu$_3$P(CO$_2$)B(C$_6$F$_5$)$_3$ in high yield (Fig. 1a). Specifically, the LB component (tBu$_3$P) interacts with the carbon atom, while the LA component (BCF) stabilizes an

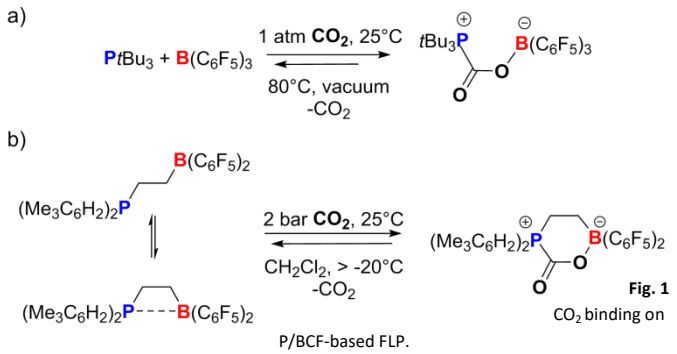

Fig. 1 CO_2 binding on

oxygen atom of CO_2 via coordination. They also showed that a pentane solution of an intramolecular FLP, $(Me_3C_6H_2)_2PCH_2CH_2B(C_6F_5)_2$, could bind to CO_2 at room temperature to form a white solid cyclo-$(Me_3C_6H_2)_2PCH_2CH_2B(C_6F_5)_2$-$(CO_2)$ with 79 % yield (Fig. 1b). The reversible nature of the CO_2 binding was demonstrated upon heating the FLP-CO_2 adducts under vacuum to 80 °C for 5 hours. Under these conditions, about half of the carbon dioxide was released and the initial FLP mixture was regenerated. These results were further supported by DFT calculations. This pioneering work offered a new metal-free approach to the activation of CO_2, which avoids the drawbacks associated with traditional metal-based catalysts. Also, it provided unprecedented insights into the fundamental chemistry of CO_2 binding by FLPs, which inspired further research in this area and led to potential applications in CO_2 capture and recycling.

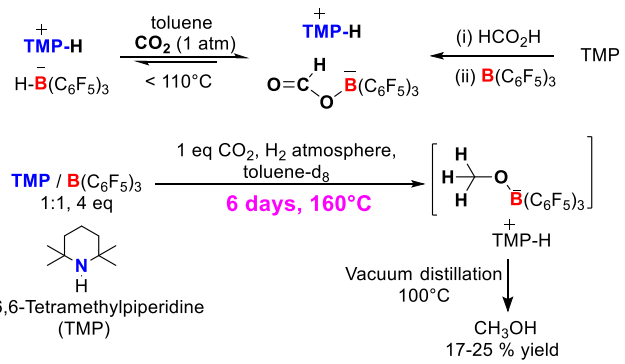

Fig. 2 Multistep FLP-mediated CO_2 hydrogenation.

In the same year 2009, Ashley *et al.* illustrated the first homogenous selective hydrogenation of CO_2 to CH_3OH using an FLP-based non-metal-mediated procedure at low pressures (Fig. 2).[31] The FLP mixture used here was a 1:1 mixture of 2,2,6,6-tetramethylpiperidine (TMP, Me_4C_5NH) and BCF which was already proven to cleave H_2 heterolytically giving a salt $[TMPH][HB(C_6F_5)_3]$ at low pressure (1-2 atm).[40] They discovered that this FLP mixture could not only cleave H_2 but also subsequently insert CO_2 in the B-H bond.

Other research groups have also employed a similar two-step mechanism, as described above, in their studies.[41,42] The vacuum distillation of the solvated methoxyborate species resulted in CH_3OH release (17-25% yield) as the only selective C1 product, along with C_6F_5H and TMP. The only source of labile protons in the decomposition reactions is provided by $[TMPH]^+$, which triggers ion

Table 1. Overview of molecular FLP systems for CO_2 reduction. Data were extracted from references when reported. (RT : room temperature)

FLP formula	LA/LB pair	Inter/Intra molecular	solvent	T, P, time	Product (Yield)	Reference
$B(C_6F_5)_3$/TMP	B/N	Inter	toluene	160 °C, 1 eq CO_2, excess H_2, 6 days	$MeOB(C_6F_5)_2$ but CH_3OH after distillation (17-25%)	31
$B(C_6F_5)_3$/Lutidine	B/N	Inter	toluene	RT, 4 atm H_2 and CO_2	[LutH] $[HC(=O)OB(C_6F_5)_3]$	43
$B(C_6F_5)_3$/amine	B/N	Inter	bromobenzene	RT, 4 atm H_2	$[PhNMe_2H][HB(C_6F_5)_3]$	44
$B(C_6F_5)_3$/*t*Bu_3P	B/P	Inter	bromobenzene	25°C, 1 bar CO_2, immediate	*t*$Bu_3P(CO_2)B(C_6F_5)_3$ (87%)	39
$(Me_3C_6H_2)_2PCH_2CH_2B(C_6F_5)$	B/P	Intra	pentane	25°C, 2 bar CO_2, 15 min	cyclo-$(Me_3C_6H_2)_2PCH_2CH_2$-$B(C_6F_5)_2$-(CO_2) (79%)	
$C_6F_4(C_6F_5))_3B/P(tBu_3)$	B/P	Inter	toluene	145 °C, 1 atm CO_2, 1 atm H_2, 24 h	[HP*t*-Bu_3] $[(C_6F_4(C_6F_5))_3BO_2CH]$	45
AlX_3 /Mes_3P	Al/P	Inter	bromobenzene	25 °C, 1 atm CO_2, 2 h	methanol (37-51 %)	46
AlX_3 /Mes_3P	Al/P	Inter	bromobenzene	RT, 2 atm CO_2, 16 h	CO, $Mes_3P(C(OAlI_2)_2O)$ (AlI_3) and $[MesPX][AlX_4]$	47
$[MeC(CH_2PPh_2)_3Cu(NCMe)][PF_6]$ / $C_{10}H_{16}N_2$ (DBU)	Cu/N	Inter	acetonitrile	80-140°C, 40 atm H_2/CO_2, 6-20 h	formate salt $[C_{10}H_{17}N_2][HCO_2]$	48
1-BR_2-2-NMe_2-C_6H_4	B/N	Intra	benzene	80 °C, 1 atm CO_2, 4 atm H_2, 9 days	formates, acetals, methoxides	32
tBu_2P–O–Al	Al/P	Intra	n-hexane	-196 °C then RT, 2 eq CO_2, overnight	*t*$Bu_2P(H)$–O–$Al(CO_2H)$	49
$K_2[(BCF)_2$-$CO_3]$	B/CO_3^{2-}	Inter	THF	160 °C, 40 bars H_2, 20 bars CO_2, 48 h	BCF-HCO_2K	50
tris(bromo)tridurylborane/DBU	B/N	Inter	acetonitrile	120 °C, 130 bar, 48 h	formate	51

recombination to form TMP and $CH_3OH{\cdot}B(C_6F_5)_3$. Dissociation of this hydroxy adduct would have led to the FLP's regeneration in a catalytic system. However, at 160 °C, the H^+ attack on the ipso-C proceeds faster, resulting in Lewis acid breakdown. As a result, inert boroxine $CH_3OB(C_6F_5)_2$ is finally formed. The identification of these key intermediates along the reaction pathway was made possible through mechanistic investigations and multinuclear solution NMR spectroscopy.

Geier and Stephan reported that the FLP based on 2,6-lutidine (Lut = 2,6-dimethylpyridine) and $B(C_6F_5)_3$ could heterolytically cleave H_2 to produce the borohydride salt, $[LutH][HB(C_6F_5)_3]$, as a white solid (Fig. 3).[52] Later, Mayer *et al.* explored the interaction of CO_2 with the same salt.[43] By treating it with 4 atm of CO_2 in toluene-d^8, they observed the formation of an air-stable white solid, $[LutH][HC(=O)OB(C_6F_5)_3]$. The reduction of CO_2 by $[LutH][HB(C_6F_5)_3]$ occurs much faster than the corresponding reaction with TMP, despite computational results by Pápai *et al.* suggesting that TMP/$B(C_6F_5)_3$ is a more reactive FLP.[53] The calculations showed that

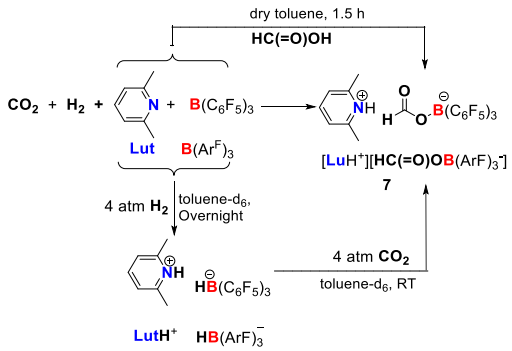

Fig. 3 Reduction of CO_2 by Lut/$B(C_6F_5)_3$ to the formato complex $[LutH][HC(=O)OB(C_6F_5)_3]$.

heterolytic cleavage of H_2 is thermodynamically less favorable for Lut/B(C_6F_5)$_3$ than for TMP/B(C_6F_5)$_3$ by approximately 10 kcal mol^{-1}. It was suggested that the higher reactivity of Lut/B(C_6F_5)$_3$ for CO_2 reduction may be due to a mechanism involving both hydride donation from [HB(C_6F_5)$_3$]$^-$ and activation of CO_2 by free B(C_6F_5)$_3$. However, preliminary studies have shown that adding excess B(C_6F_5)$_3$ did not significantly accelerate the reaction, and adding excess lutidine also did not cause any substantial change in rate.

Afterwards, Voss and coworkers examined how different amines (N-dimethylaniline, N-isopropylaniline, 1,4-C_6H_4(CH_2NHtBu)$_2$, and benzyldimethylamine) react with BCF and explored their FLP behavior.[44] They illustrate how both steric and electronic factors influence the formation of LP adducts. Although these factors may hinder adduct formation, they allow access to free FLPs that can be used for further reactions. Additionally, the borane's hydridophilic nature promotes the formation of minor side products that are derived from hydride abstraction from the α-C to produce iminium salts. They further studied the reaction of H_2 and CO_2 with these pairs. The Lewis pair of N-dimethylaniline−B(C_6F_5)$_3$ reacted quickly with 4 atm H_2 at 25 °C, even though the LB component had low basicity. By the heterolytic cleavage of H_2, it produced the ammonium−hydridoborate salt [PhNMe_2H][HB(C_6F_5)$_3$]. The CO_2 adducts of such salts have been investigated by Erker *et al.* as discussed above and were found to be thermally unstable, releasing CO_2 quickly in solution at temperatures ranging from -20 to +80 °C.[39,54]

The following year, Travis *et al.* focused specifically on FLPs based on the Lewis acids tris(perchloroaryl)borane (BArCl) and tris(2,2′,2′′-perfluorobiphenyl)borane (PBB) with selected phosphines, which were extensively studied for small molecules activation.[45,55,56] The reactivity was found mainly driven by the activation of H_2 before a concerted addition of CO_2. The Lewis acidity of the catalyst is crucial in this process, as it needs to be strong enough to split H_2 but not too strong to allow hydride transfer to CO_2. They designed Lewis acid assuming that the steric bulkiness at the ortho position could decrease the B-O bond strength of the methoxyborate formed and could consequently facilitate its cleavage to evolve methanol and regenerate the FLP catalyst. Such sterically congested LA was found less effective in activating H_2 despite having higher Lewis acidity. This was mainly ascribed to the steric hindrance around the boron center, hindering the approach of H_2 and increasing the energy barrier for the reaction.

Among all the phosphines tested with BArCl, only P(tBu)$_3$ and P(Cy)$_3$ could cleave H_2 without thermal decomposition and were found to be the most active, completing the reaction in a long time of 56 and 40 hours at 90°C respectively. The formatoborate [PBB-OC(O)H][H-P(tBu)$_3$] was prepared by exposing the [PBB-H][H-P(tBu)$_3$] salt to one atmosphere of CO_2. Still, the reaction did not occur at room temperature but required heating at 140°C for several days.

2.1.2. Intermolecular FLPs based on other metal-based Lewis acids

In contrast to previous reversible systems, Menard and Stephan reported in 2010 FLPs based on aluminium AlX_3 (X = Cl or Br) with $PMes_3$ (Mes = 2,4,6-$C_6H_2Me_3$) which could irreversibly bind CO_2. This system could further produce methanol at room temperature in the presence of excess ammonia borane as a hydrogen source (Fig. 4).[46] The CO_2 sequestered species $Mes_3PC(OAlX_3)_2$ (X = Cl or Br) was stable and obtained with yields up to 83%. The corresponding CO_2 adducts were stable up to 80°C under vacuum, despite having lower Lewis acidic and basic components than other similar compounds that rapidly lose CO_2 at much lower temperatures.[39] Quenching with H_2O led to the isolation of CH_3OH in 37–51% yield, representing a further example of the stoichiometric reduction of CO_2 to CH_3OH. However, no mechanism of this reduction reaction was reported. Since then, and over the last decade, Stephan and co-workers widely studied various FLPs for CO_2 activation and/or reduction following a similar methodology.[8,57–60]

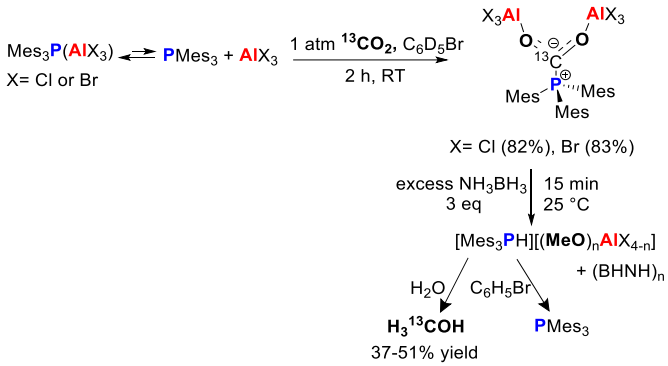

Fig. 4 Reactivity of Al/P FLP towards CO_2 and subsequent reduction reaction.

The same group demonstrated that P/Al/CO_2 adducts can also be used as a means to reduce CO_2 to CO.[47] Berke *et al.* used transition metal-based FLPs in the hydrogenation of CO_2 in 2013.[61] The authors showed that 0.5 mol% of ReHBr(NO)(PR_3)$_2$ and B(C_6F_5)$_3$ in the presence of $C_5H_6Me_4NH$ catalyzed the formation of formate salt [$C_5H_6Me_4NH_2$][HCO_2]. Similarly, in 2015, Zall *et al.* reported the CO_2 hydrogenation catalyst based on a well-defined copper complex with triphos ligand 1,1,1-tris-(diphenylphosphinomethyl)ethane.[48] The [MeC(CH_2PPh_2)$_3$Cu (NCMe)][PF_6] complex acted as a Lewis acid in the presence of $C_{10}H_{16}N_2$ (DBU) base, H_2, and CO_2 to generate the salt [$C_{10}H_{17}N_2$][HCO_2].

2.1.3. Intramolecular FLPs based on Al or B Lewis acid

After reporting the reduction of CO_2 using amphiphilic FLPs in the presence of hydroboranes giving methoxyboranes,[62–65] Fontaine *et. al* described in 2015 intramolecular FLPs containing B and N as Lewis pairs.[32] Instead of using BCF with high Lewis acidity, they explored less acidic systems containing tri-aryl boron centers. Like Menard and Stephan in 2010 for intermolecular systems using Al/P FLP pairs,[46] Mitzel *et al* recently reported FLP based on Al/P bridged by geminal oxygen.[49] Bis_2AlH (Bis = CH($SiMe_3$)$_2$) and tBu$_2$P(O)H were reacted to form an adduct of phosphane and alane, tBu$_2$P(H)-O-Al(H)Bis_2 (

Fig. **5**). Due to the high reactivity of the latter releasing H_2, its reaction with CO_2 was performed at -196 °C. This allowed achieving a stoichiometric reduction of CO_2, resulting in the formation of stable aluminium formate. Despite its appealing reactivity, this FLP system could not be used as a catalyst for the hydrogenation of CO_2 as the H_2 adduct was found to be in equilibrium with free H_2 and the CO_2 adduct was too stable.

More recently, Fernández, Breher and co-workers reported a “hidden FLPs” based on a five-membered ring phosphorus ylide containing aluminium or gallium as a LA site.[66] This system was

shown to reduce CO_2 to methanol in the presence of borane as a reducing agent and upon the addition of water.

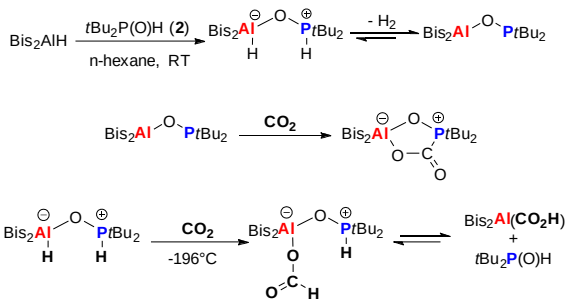

Fig. 5. Reactivity of Al-O-P FLP towards H_2 and CO_2 to formic acid adduct.

2.1.4. Emerging catalytic molecular FLPs for CO_2 hydrogenation.

Towards the catalytic application of FLPs, a seminal work by Stephan and coworkers in 2014 reported the combination of P(*t*Bu)$_3$ as Lewis base in a catalytic amount with an excess of 9-borabicyclo(3.3.1)nonane (H-BBN) as Lewis acid. Based on borane consumption, TONs of 5500 were reached for the CO_2 activation to methoxy-borane (MeO-BBN) with 98% selectivity in bromobenzene solvent under 5 atm. at 60°C (Fig. 6).[67]

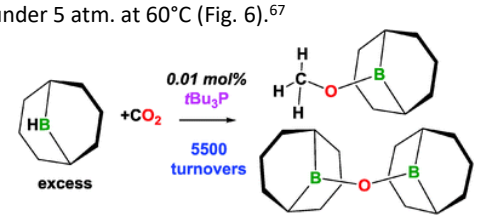

Fig. 6 Catalytically active Lewis base in FLP-driven CO_2 activation.

Later in 2018, Zhao *et al.* described a similar "semi-catalytic" CO_2 hydrogenation to formate using a catalytic amount of BCF as LA and an excess of carbonate base M_2CO_3 (M = Na, K, and Cs).[50] This system resulted in the formation of a Lewis pair (K_2-[(BCF)$_2$-CO_3]) that can react with both H_2 and CO_2 to produce the BCF- HCO_2M (Fig. 7). Using a 10'000-fold excess of base compared to BCF, under CO_2:H_2 = 20:40 bar, in THF for 48 hours at 160 °C, they could reach a TON of 4'000 based on the moles of formate produced per mole of BCF.

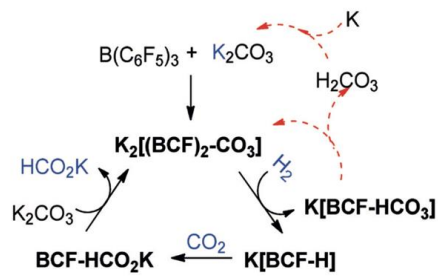

Fig. 7. Proposed catalytic process for the hydrogenation of CO_2 using K_2-[(BCF)$_2$-CO_3]. Reproduced from ref 50. Copyright 2019 Wiley-VCH.

More recently, in 2022, Dyson and Corminbœuf used linear scaling relationships to explore FLPs combinations for direct hydrogenation of CO_2.[51] Thousands of FLPs combinations were computationally screened based on the acidity and basicity of the individual components. Their computational approach and results are discussed in more details in Section 3.2.2. In short, the authors showed that balancing the cumulative strength is key to catalytic performance. From the wide set of FLPs explored, those consisting of tris(*p*-bromo)tridurylborane (tbtb)/DBU with a weak LA and B-Me_2F_2/pyridine with a weak LB were found to be the most effective ones. Their predicted high activity results from their ability to provide a suitable balance between the limiting steps, i.e. activation of H_2 and release of the product. Notably, the tbtb/DBU-based FLP was found to experimentally catalyze the direct hydrogenation of CO_2 to formate. It occurs in the presence of 100 equivalents of the base compared to the acid at a very high pressure of 150 bar (25 bar CO_2 and 125 bar H_2) at 120°C after 48 hours (Fig. 8). TON of 24 were obtained, and, noteworthy, the product of the reaction was the formate salt of the Lewis base. They also explained the reason why previous attempts to use molecular FLPs for CO_2 hydrogenation combining strong LAs like BCF with various nitrogen-containing bases (such as TMP or lutidine) resulted in boroformate salts with no product release. The authors concluded that the formate release step would always be the limiting factor and prevent catalytic turnover, no matter which base is chosen when such a strong LA is used.

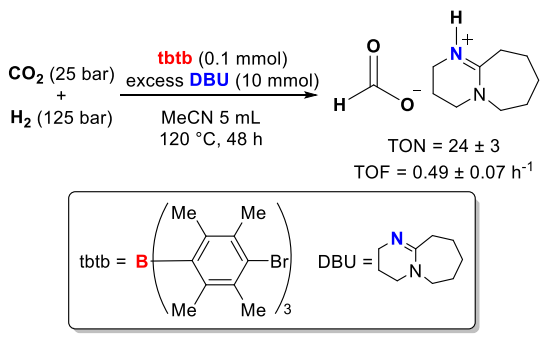

Fig. 8 Catalytic hydrogenation of CO_2 to formate using tbtb/DBU system. Adapted from ref 51. Copyright 2022 Wiley-VCH.

2.2. FLPs heterogenization in porous solids for CO_2 hydrogenation

Although FLP systems are renowned for their metal-free nature and great reactivity and selectivity, their immobilization into porous support has been driven by the aim to enhance their stability against deactivation. Immobilization would also in principle allow better control of acid-base distances, a key parameter, especially for CO_2 activation.[68] Furthermore, the heterogenization of FLPs within porous solids should enable their implementation in continuous flow processes, also key for CO_2 valorization at a large scale. While the field of homogeneous FLPs has benefited from the great knowledge gained over the last decade,[12,13] the transfer of FLPs' chemistry to heterogeneous catalysis is very recent and remains challenging.[14,15] We gather here examples of molecular FLPs heterogenization on various supports for CO_2 and/or H_2 activation (Table 2).

Table 2. Overview of heterogenized FLP systems for CO_2 and/or H_2 activation. Data were extracted from references when reported. (RT: room temperature).

FLP type	LA/LB pair	Inter/Intra molecular	solvent	T, P, time	Product (Yield)	Reference
$HB(C_6F_5)_2$ / PPh_3@silica	B/P	Inter	pentane	80 °C, 40 bar H_2, 4 h	$[\equiv(SiO)_2Al(OEt)(OC_6H_4PH(C_6H_5)_2)]$ $[HB(C_6F_5)_2]$	69
BCF@silica / tBu$_3$P	B/P	Inter	toluene	65 °C, 2 bar H_2, 72 h	$[\equiv SiOB(H)(C_6F_5)_2][t Bu_3PH]$	70
PR_3@silica / BCF PR_3 / BCF@silica	B/P	Inter	pentane, toluene	RT to 60 °C, 2 bar H_2, 2 bar CO_2, 48 h	formic acid	71
$B(C_6F_5)_2$(Mes) / DABCO@MOF	B/N	Inter	toluene	RT, 10 bar H_2, 48 h	α, β-unsaturated amine	72
$B(C_6F5)_3$ / DABCO@MOF	B/N	Inter	toluene	80 °C, 60 bar H_2, 24 h	alkylidene malonate (88-95%)	73
B-MOF / amine	B/N	Inter	acetonitrile	120 °C, 10 bar CO_2, 24h	benzimidazoles	74
$B(C_6F_5)_3$ / MOF(porphyrin)	B/N	Inter	toluene	RT to 100 °C, 20 bars H_2 and CO_2, 21 h	$[(MeO)B(C_6F_5)_3]$ then MeOH after hydrolysis	75
$B(C_6F_5)_3$ / diamine@MOF	B/N	Inter	toluene	RT, 20 bar H_2, 48 h	amine	76
BCF / P-POP	B/P	Inter	cyclohexane	RT, 6 bar H_2	$[(Ar)_3PH][HB(C_6F_5)_3]$	77
BCF / N-POP	B/N	Inter	toluene	80 °C, 60 bar H_2, 24 h	diethyl-2-benzylmalonate	78
P-POP / B-POP	B/P	Inter	toluene	60 °C, 1 atm CO_2	formamide	79

2.2.1. Immobilization in siliceous porous solids.

Taoufik *et al.* reported in 2016 a strategy to support triphenylphosphine and $HB(C_6F_5)_2$ FLP on silica.[69] The grafting of the phosphine was accomplished by reacting (4-hydroxyphenyl)biphenyl with $\equiv(SiO)_2Al(i Bu)(OEt)$ in ether at room temperature for 12 hours. The resulting silica-supported LB was exposed to the benzene solution of $HB(C_6F_5)_2$ or BCF for 3 hours at room temperature to achieve the semi-immobilized FLP on silica support (Fig. 9). The same year, O'Hare reported a synthesis of silica-supported BCF ($\equiv$SiO-$B(C_6F_5)_2$, s-BCF) and then combined it with tri-*tert*-butylphosphine as LB to form a solid-phase $[\equiv SiO\text{-}B(C_6F_5)_2][t Bu_3P]$.[70] This FLP was shown to cleave H_2 heterolytically in toluene at 65°C for 72 hours to give $[\equiv SiO\text{-}B(H)(C_6F_5)_2][t Bu_3PH]$. Additionally, this FLP was shown to activate polar O-D bonds at room temperature. In 2018, the group of Zhang described the semi-heterogenization of Lewis pairs on silica.[80] A silicon wafer functionalized with N-heterocyclic olefin as LB was shown to initiate lactones polymerization in the presence of tris(pentafluorophenyl)alumane as LA, giving linear polymer brushes. In 2020, Erasmus *et al.* reported a new approach to graft FLP on hydroxylated silica nanopowder.[71] They grafted triethoxysilane derivatives of Lewis acid and bases on the hydroxylated silica nanopowder which could interact with their respective LB and LA components to form FLPs. These silica nanopowder-supported LA and LB could activate H_2 when exposed to their complementary FLP partners (2 bar, room temperature, 3 days) and subsequently transform CO_2 into HCOOH (2 bar, 60°C, 3 days) (Fig. 10).

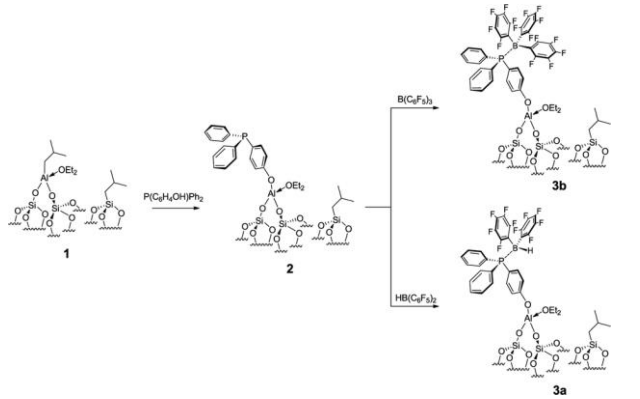

Fig. 9 Formation of silica-supported phosphine Lewis base combined with solubilized Lewis acids. Reprinted from ref 69.

Fig. 10 CO_2 capture by silica-supported LA and dissolved LB mixture. Reprinted from ref 71. Copyright 2020 American Chemical Society.

2.2.2. Immobilization in ordered metal-organic and covalent organic frameworks.

Metal-organic frameworks (MOF) already demonstrated their appealing properties for CO_2 capture and conversion.[81–85] Thanks to their hybrid organic-inorganic nature, their tunability of the pore sizes, a large variety of topologies and their high crystallinity and high porosity,[86,87] MOFs are ideal candidates for the heterogenization of FLPs. Indeed, crystalline-ordered networks, with regularly distributed functional groups, can allow precise control over the positioning of FLP partners, critically related to the FLP activity.

Since 2015, several computational studies have proposed the possibility of creating MOF-based FLP catalysts.[88–93] However, only in 2018 the Ma's group achieved experimentally the introduction of FLPs into MOF in a semi-immobilized manner.[73] The Cr-MIL-101 was selected as an adequate MOF platform due to its large open porosity and the presence of Cr open metal sites.[94] The selected classical FLP comprises BCF as the LA and 1,4-diazabicycl[2.2.2]octane (DABCO) as a potent LB. One of the N atoms in DABCO coordinated to the open metal site of the MOF and the second N atom paired BCF simultaneously as illustrated in Fig. 11). Although the obtained Cr-MIL-101-LP was not reported for CO_2 hydrogenation, the solid efficiently catalyzed the reduction of C=N imine bonds with up to 100% yield using HBpin as a reducing agent, as well as the direct hydrogenation of alkylidene malonates under 60 bars H_2 for 24 hours at 80°C giving up to 91% yield. This catalyst was recyclable for up to seven runs for the reduction of imines.

The following year, in 2019, the same group reported the chemoselective catalytic hydrogenation of α, β-unsaturated imine compounds under 10 bar H_2 at room temperature in high yields up to 100% using the same Cr-MIL-101 MOF.[72] The FLP anchored in the MOF was $B(C_6F_5)_2(Mes)$/DABCO following the same strategy.[73] Interestingly, this immobilized FLP could activate H_2 forming MIL-101(Cr)-FLP-H_2 at room temperature and hence, forming an ammonium hydridoborate salt, $[CH(CH_2CH_2)_3NH]$ $[HB(C_6F_5)_2(Mes)]$. Powder XRD was used to confirm the retention of the structural integrity of MIL-101(Cr)-FLP-H_2, its surface area being of 1120 m^2g^{-1} as obtained by N_2 sorption studies. The MIL-101(Cr)-FLP displayed the same productivity for the imine reduction for up to five runs.

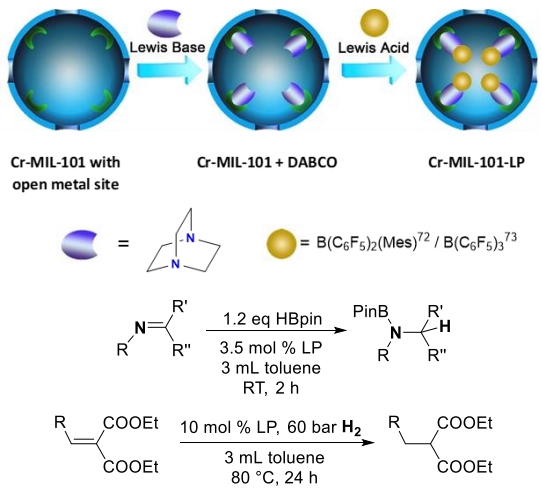

Fig. 11 Synthesis of Cr-MIL-101-LP as a catalyst for C=C and C=N reduction reactions. Adapted from ref 73. Copyright 2019, with permission of Elsevier.

Dyson and Stylianou and co-workers reported a water-stable MOF named SION-105 which incorporated a bulky LA-functionalized ligand.[74] MOF SION-105 was synthesized by the combination of Eu-$(NO_3)_3$ and tris(p-carboxylic acid)tridurylborane (H_3tctb) in a 2:1 mixture (Fig. 12). SION-105 allowed for the *in situ* formation of FLP by employing Lewis basic diamine substrates which could be efficiently transformed to benzimidazoles in the presence of excess silane and 10 bar CO_2 as a C1 source at 120° C for 24 hours, with isolated yields up to 90%.

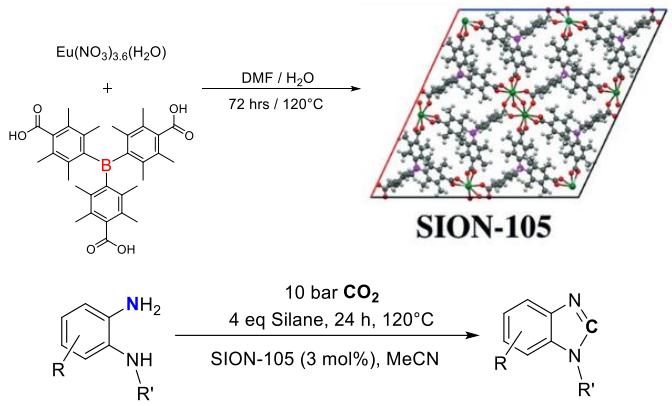

Fig. 12 Synthesis of SION-105 and the reaction of aromatic o-diamines with CO_2 in the presence of SION-105. Reprinted with permission from ref. 74. Copyright 2020 Wiley-VCH.

In the same year, the same group conducted another study on stoichiometric CO_2 fixation using an inverse approach.[75] Using the MOF-545, which contains Zr_6O_8 clusters linked by tetrakis(4-carboxyphenyl)porphyrin (TCPP) ligands, nitrogen atoms in porphyrin act as LB and formed an *in situ* FLP when combined with the BCF LA introduced as a guest molecule (Fig. 13).

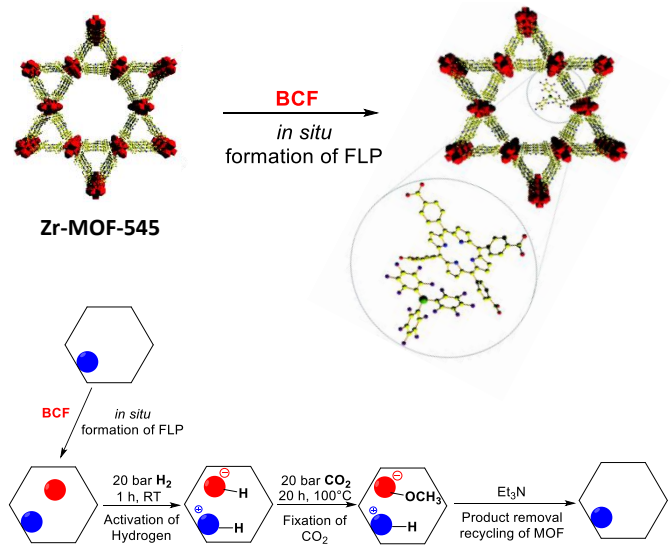

Fig. 13 BCF-impregnated MOF-545 for CO_2 fixation.

The BCF@MOF-545 was subjected in toluene to 20 bars of H_2 at room temperature for 1 hour and then to 20 bars of CO_2 at 100°C for approximately 20 hours. Following this procedure, the formation of methoxyborate, $[(MeO)B(C_6F_5)_3]^-$ was observed along with the side

products methoxyborate and the hydroxyborate, $[(HO)B(C_6F_5)_3]^-$, which were confirmed by mass spectrometry and NMR. During the experiment, the decomposition of the products into $[(MeO)B(C_6F_5)_2]$ and C_6F_5H was observed. These products could potentially give methanol upon hydrolysis. Notably, the MOF remained intact even after three runs. Although the NMR analysis showed the presence of the hydrogenated products, these were not quantified.

With a similar approach as in 2019, Ma's group developed a molecular chiral catalyst by incorporating chiral FLPs (CFLPs) into achiral MOFs for asymmetric hydrogenation of imines.[76] Guided by a computational screening, the 2,5-dihydro-3,6-dimethoxy-2-isopropylpyrazine bifunctional basic amines were selected to coordinate the Cr(III) open site with one N atom and paired with BCF. The presence of the FLP was confirmed by elemental analysis, FTIR, XPS, EDS and ^{11}B NMR comparison of CFLP@MIL-101(Cr)-H_2 and BCF. When applied to the asymmetric hydrogenation of imines (20 bars of H_2, 48 hours at room temperature) this catalyst gave yields above 95% in most of the different imines with enantiomeric excess up to 85%.

More recently, in 2022, a COF functionalized with FLP was reported by Hu's group.[95] Inspired by the catalytic activity of triaryl phosphine and BCF pair, they developed COF@FLP by the post-synthetic modification of the crystalline brominated COF with triaryl phosphine unit as Lewis base by cross-coupling reaction, followed by the encapsulation of BCF as Lewis acid. These COFs were used for the stereoselective hydrogenation of alkynes into Z-alkene with H_2 and effectively recycled for up to ten runs.

2.2.3. Immobilization in disordered organic polymers

In 2017, the first microporous polymer networks based on tris(2-methylphenyl)phosphine and tris(2,6-dimethylphenyl)-phosphine were reported by Thomas *et al.* which contained the LB component of the FLP in its structure (Fig. 14).[77] Polymers were shown to rapidly absorb BCF by swelling when they were suspended in a DCM solution of BCF to form a semi-heterogenized FLP. Fluorescence experiments under UV irradiation clearly showed the quenching of the fluorescence for the polymers due to the interaction with BCF. Solid-state ^{31}P MAS NMR spectroscopy also confirmed the presence of P/B FLP. These polymers were proven capable of H_2 activation at room temperature via H/D isotope scrambling experiments under a 6 bar H_2/D_2 mixture at room temperature.

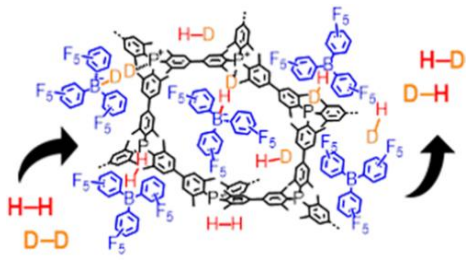

Fig. 14 BCF-impregnated phosphine-based polymer for H_2 cleavage. Reprinted with permission of ref 77. Copyright 2017, American Chemical Society.

Similarly, in 2018, Rose *et al.* reported a polyamine organic framework with tertiary amine as LB sites, which forms *in situ* FLP when exposed to BCF in solution.[78] The impregnation of BCF was studied by ATR IR spectroscopy showing a new IR band at 1276 cm^{-1} corresponding to the B-N interaction between BCF and polyamine. As a semi-heterogenized FLP, this polymeric amine in combination with BCF was shown to cleave H_2 heterolytically, as confirmed by ^{11}B NMR, and applied in the catalytic hydrogenation of electron-poor diethyl benzylidenemalonate.

Following a strategy based on fully covalently immobilized FLP, Yan and coworkers reported the physical mixture of two linear polymers functionalized with either BCF derivative (LA) or triarylphosphine (LB) as illustrated in Fig. 15.[79] Upon CO_2 exposure under 1 atm. in toluene, the intermolecular polymeric FLP is assembled to form micelles with bridging CO_2 between polymer chains. These micelles were shown to be nanocatalysts for the secondary amine formylation with TON up to 15000 in the presence of phenylsilane as a reducing agent, with efficient recycling for up to eight catalytic runs.

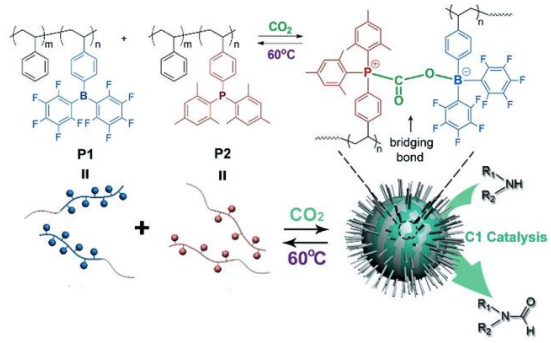

Fig. 15 Self-assembled FLP-polymer micelles for CO_2 activation. Reprinted with permission from ref 79. Copyright 2018, WILEY-VCH.

From siliceous materials to MOFs, COFs and POPs, the above-reviewed studies evidence that the vast majority of heterogeneous FLPs are actually semi-heterogenized FLPs. As such, they consist of solids made around or functionalized with one FLP partner, while the second partner is non-covalently impregnated within the solid. Such semi-heterogenization strategies might lead to the leaching of one of the partners thus limiting the durability, and the subsequent productivity, of these however promising systems. The fully covalently heterogenized FLPs were based either on phosphine-functionalized metallated silica[96] or on the physical mixture of two polymers functionalized respectively with one FLP partner,[79] with however ill-defined and randomly distributed active sites as well as questionable utilization of the bulk FLP-functionalized solids. Furthermore, although the reported FLP-containing solids were demonstrated to efficiently activate either H_2 or CO_2, none of them were shown to perform direct CO_2 hydrogenation so far.

3. Learnings from computational chemistry

The rational design and development of efficient FLP-based catalysts for CO_2 hydrogenation requires a comprehensive understanding of the intricate relationships between molecular structures and their catalytic functionalities. This entails delving into the catalytic properties of molecular FLPs, while also rationalizing the conformational and environmental effects that govern their integration into the porous framework of materials. In this regard, quantum mechanical calculations have been extensively employed to: i) obtain atomistic insights into the activation pathways of both

H_2 and CO_2; ii) identify the factors that influence their performance; and iii) evaluate the potential impact of their immobilization inside porous matrices. This section covers the most relevant computationally-derived advances in this direction, ultimately aiming to predict and drive the synthesis of efficient FLP-based catalytic systems. Sections 3.1 and 3.2 summarize the main findings inferred from studies on molecular FLPs, while section 3.3 delves into *in silico* studies on heterogenized FLP systems.

3.1 H_2 splitting in molecular FLPs: a generally accepted initial step

The hydrogenation of CO_2 by FLPs has been often shown to require the initial generation of an active hydrogenating species. This can be achieved via the heterolytic splitting of a H_2 molecule into a hydride and a proton, which are accommodated on the LA and LB centers conforming the FLP, respectively. Beyond CO_2 hydrogenation purposes, the splitting of H_2 by FLPs represents an interesting process *per se*, playing a central role in the hydrogenation of a variety of unsaturated compounds.[26] Besides, the ability to split H_2 under mild conditions confers FLPs the potential to be used as molecular platforms to store H_2 fuel in a safe and easy-to-handle manner. On these grounds, extensive theoretical have been devoted to understanding the reactivity of FLPs towards H_2 and the factors that govern it. This section aims to give a brief overview of the most relevant computationally-derived findings in this sub-area, as well as the current controversies and challenges. For a more comprehensive review of computational studies on H_2 splitting by FLPs, please refer to the Supporting Information. Also, an extensive array of experimentally tested cases involving H_2 splitting by FLPs has been explored employing computational methods (see SI for details). These efforts have contributed to the establishment of a well-defined mechanistic picture depicted in Fig. 16 and are summarized as follows.

On the one hand, *intermolecular* FLPs proceed via the formation of a non-covalent adduct between the LA and LB partners also referred as an "encounter complex". This is followed by the insertion of H_2 into the reactive pocket and its splitting to form a hydrogenated $[LB\text{-}H]^+\cdots[LA\text{-}H]^-$ ion pair.

On the other hand, *intramolecular* FLPs may either activate H_2 by themselves or dimerize to operate as an intermolecular FLP. The competition between intra- and intermolecular pathways in intramolecular FLPs has not been systematically investigated for a whole range of systems. Thus, setting clear conclusions about the factors that determine their relative likelihood remains challenging. Still, the prevalence of each of these paths might depend on the equilibrium LA···LB distance within the intramolecular FLP and on the ability of FLPs to dimerize into stable non-covalent adducts. Up to now, this mechanistic knowledge has been successfully applied to rationalize the H_2 splitting activity of a wide variety of FLPs, including mostly P/B[98–116] (known as thermally-induced FLPs[53,117]) N/B pairs,[29,97,113,115,118–123] and less often carbene/B[124] and N/TM (TM = Ni, Pt) pairs,[125] or even that of heterogeneous systems such as hydroxylated indium oxide surfaces.[126–128]

Computational efforts have been devoted to identify the key factors that govern the H_2 splitting, aiming at establishing structure-activity relationships and clear design rules. The primary structural requirement of an active FLP is to offer a suitable LA···LB distance. For instance, Vankova and co-workers determined that optimal P···B distances for H_2 splitting lie within a range of 3 to 5 Å by performing constrained potential-energy surface scans along the P···B distance of a $P(t\text{Bu})_3/B(C_6F_5)_3$ FLP.[129] As for B/N FLPs, Corminbœuf and co-workers identified that the optimal B···N distance for H_2 splitting is ca. 2.9 Å. Still, the range of distances in which the energy of the TS varies within an energy range of 5 kcal mol^{-1} spans from ca. 2.6–3.5 Å.[68] Thus, when targeting the heterogenization of FLP systems, it is essential to ensure that the positioning of the LA and LB partners within the material does not impose a suboptimal LA···LB separation.

Another key factor in FLPs' reactivity is the electronic properties of the substituents of both LB and LA centers, affecting their basicity and acidity, respectively. A first attempt to set relationships between such molecular features of FLPs and the H_2 splitting free energy (indicating its thermodynamic feasibility) was proposed by

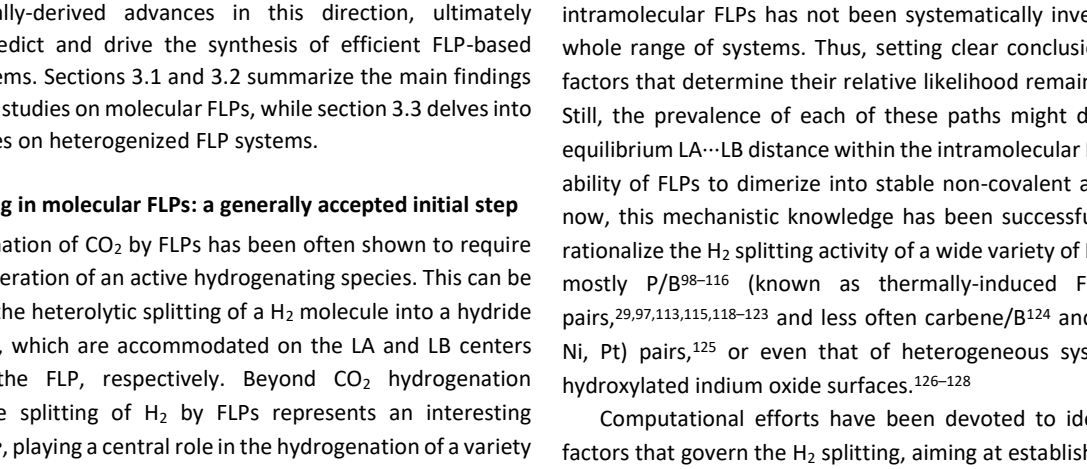

Fig. 16 Overview of the main reaction mechanisms characterized by DFT calculations to govern the H_2 splitting by (a) intramolecular and (b) intermolecular FLPs. 3D-structures on the right show representative transition-state geometries for: H_2 activation by (c) intramolecular FLPs through an intramolecular path. Reprinted with permission from ref 97. Copyright 2016, Wiley-VCH; (d) intramolecular FLPs through an intermolecular path. Adapted from ref 98 with permission from the PCCP Owner Societies; (e) an intermolecular FLP. Reprinted with permission from ref 99. Copyright 2008, Wiley-VCH.

Pápai and co-workers.[53] They carried out a comprehensive computational investigation using a series of intra- and intermolecular FLPs, which led to several conclusions, which were further supported by other works (see SI for details):[97,129,123,114]

i) the thermodynamics of the H_2 splitting correlates with the *cumulative acid-base strength* of the FLP partners, which can be quantified from proton and hydride attachment energies;

ii) linked or intramolecular FLPs benefit from a smaller entropic penalty along the reaction coordinate than intermolecular FLPs and thus, require smaller cumulative acid-base strengths to be active;

iii) reaction free-energies for H_2 splitting by the analyzed set of intramolecular FLPs was correlated inversely with the LA···LB distance. In other words, the shorter the donor-acceptor distance is, the more exergonic the H_2 splitting is.

Ye and Johnson further proposed an original approach to explore computationally the immobilization of intramolecular FLPs for CO_2 hydrogenation in UiO-66, a porous MOF matrix.[89] They aimed to set the very first structure-activity relationships between the structure of molecular FLPs and their ability to activate H_2 and hydrogenate CO_2 in the H_2/CO_2 gas stream. Here, we focus on their findings on the initial H_2 splitting step, while CO_2 hydrogenation will be discussed in section 3.3. The authors selected a set of 8 B/N FLPs, which on paper, can be covalently grafted on the terephthalate linkers of UiO-66 (Fig. 17a). These consist of a pending pyrazole functionalized with a BR_2 moiety that leads to a series of B/N FLPs of increasing acidity by varying R. Computing electronic energy profiles for all systems, the authors tried to find Brønsted–Evans–Polanyi (BEP) relationships[130,131] between energetic parameters (reaction energies and barriers) and a set of molecular descriptors. The latter include the acidity of the LA, the basicity of the LB, the electronegativity, chemical hardness and softness of the FLP sites, atomic charges and structural parameters of both the bare FLP and the zwitterionic hydrogenated intermediate.

The H_2 dissociative adsorption energy (i.e. heterolytic splitting of H_2) was found to correlate linearly with the hydride attachment energy (Fig. 17b).[89] As the LA strength increases, so does the H_2 dissociative adsorption energy. Notably, no correlation was found with the proton attachment energy, in line with the experimental findings of Berke and co-workers.[132] Still, we can note this computational work only addressed the impact of the substituents at boron (LA) center, resulting in a rather narrow range of proton attachment energies. The analyzed FLPs do not significantly differ in terms of LB basicity, leaving the impact of the latter uncharted.

Another linear BEP relationship was identified between the H_2 splitting energy barrier and the LA chemical hardness.[89] Increasing the hardness of the LA decreases the barrier for H_2 splitting in accordance with Pearson's theory. We wish to stress here that, unlike the H_2 adsorption energy, this barrier did not correlate with the acidity of the LA. The BEP principle thus does not fully apply to the H_2 splitting process, given the absence of a linear correlation between reaction energies (thermodynamics) and barriers (kinetics). The other BEP relationship found between the H_2 splitting barrier and the bond angle formed by N_b, N_a and B centers in the bare FLP was ascribed to the fact that larger angles induce strain in the FLP, which lowers the barrier. It is also relevant for the present review that the MOF environment was found to marginally affect the adsorption energy of H_2 on the FLP, as similar reaction energies were obtained from both isolated and in-MOF FLP models.

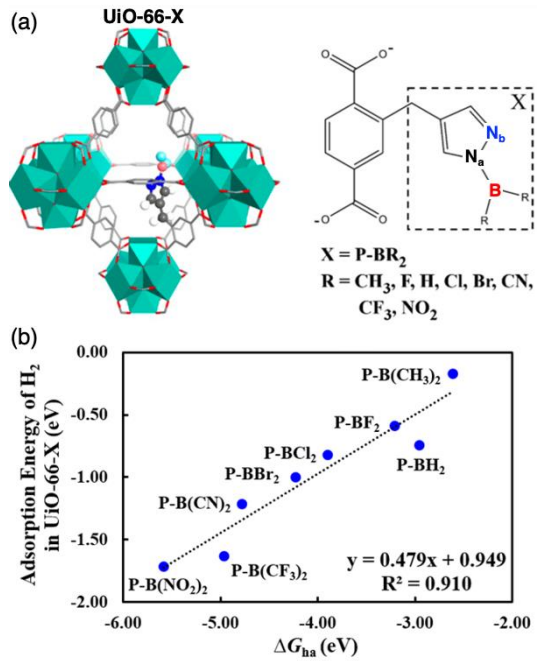

Fig. 17 (a) Octahedral cage of the UiO-66 Metal-Organic Framework bearing a linker functionalized with a Lewis Pair (X). (b) Adsorption energy of H_2 in UiO-66-X plotted against the free-energy of hydride attachment to the B center of the Lewis pair. Reprinted with permission from ref 89. Copyright 2015, Wiley-VCH.

Two years later, Ye *et al.* revisited the factors that influence the thermodynamics and kinetics of H_2 splitting on FLPs grafted in UiO-66 by enlarging their study to four families of intramolecular FLPs including B/N and B/P pairs attached to structurally distinct molecular scaffolds.[91] Although quantitative linear correlations between H_2 splitting energies and hydride attachment-free energies were found again for each FLP family (with r^2 >0.95), as shown above, they did not apply for all FLP families taken together (r^2 =0.834). This evidenced that besides hydride attachment-free energies, other factors influence the binding energy of H_2. An in-depth screening of molecular descriptors, revealed that it is also proportional to the LA···LB distance in the bare FLP and to the variation of the angles concerning the LA/LB sites and the two consecutive atoms of the scaffold in the direction of the FLP partner upon H_2 binding.

Overall, despite the complexity of FLP's reactivity, computational methods have significantly contributed over the years to the generation of valuable knowledge that can be used to guide the experimental design of FLPs to conduct H_2 splitting. Still, several points lack a quantitative unambiguous answer. For instance, the exact structural and electronic parameters that determine whether an intermolecular FLP operates through an intra- or an intermolecular mechanism are yet to be understood. Other aspects of the H_2 splitting by FLPs that remain controversial or unclear nowadays are the relative weights of the impact of electric field polarization and orbital overlap on H_2 splitting, as well as those of LA and LB strengths and how they relate to the FLP's nature and

structure (see Fig. S6 and related text in SI). Also, although a set of molecular parameters of FLPs have been recognized to influence H_2 splitting kinetics and thermodynamics, generic and quantitative structure-activity relationships are still to be established. Most likely, this is because, besides eventual exceptions, the series of FLPs analyzed in each work are constrained to a single family of FLPs and quite often, account for a rather limited number of structures.

More importantly, within the present context of using FLPs not only for H_2 splitting but also for subsequent hydrogenation of CO_2, balancing the energetics of H_2 splitting with those of the subsequent hydrogenation step is crucial. Specifically, FLPs should bind H_2 strongly enough to make the H_2-splitting step feasible, but not too strong so as to preclude subsequent hydride/proton transfer to an incoming CO_2, molecule. In other words, a too strong Lewis base/acid would produce a too weak Brønsted acid/hydride donor, hampering CO_2 hydrogenation. This adds an extra layer of complexity to the design challenge: the goal is drifted from minimizing energy barriers while favoring thermodynamics for each single elementary step process to identifying the molecular descriptors and the sometimes-overlooked experimental conditions that simultaneously optimize the performance of two distinct processes.

3.2 Molecular FLPs for CO_2 hydrogenation

Carbon dioxide is an exceptionally stable molecule and its activation and conversion are hence not straightforward. The ability of FLPs to heterolytically split H_2 and subsequently hydrogenate organic compounds has prompted the exploration of the potential use of FLPs for the direct hydrogenation of CO_2 with H_2 following the two-step process shown in Scheme 1.

Scheme 1. FLP-mediated CO_2 hydrogenation mechanism.

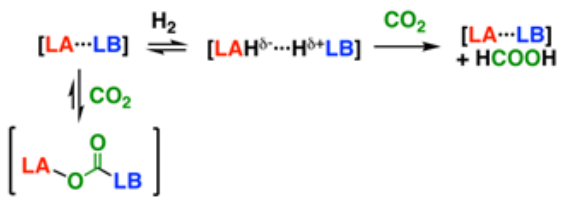

However, CO_2 can be also captured by FLPs as shown in section 1 and hence, compete with H_2 for FLP sites.[13] Notably, FLPs often bind CO_2 more strongly than H_2, which may hamper H_2 splitting as the first step of CO_2 hydrogenation because of an additional energy penalty associated to CO_2 release. Still, such FLP-CO_2 adducts are not necessarily detrimental for CO_2 hydrogenation, as they could allow distinct mechanistic scenarios, as discussed in detail below.

3.2.1. Computational mechanistic studies on FLP-promoted CO_2 hydrogenation.

Early mechanistic computational studies were performed on systems that leverage the aforementioned ability of FLPs to capture CO_2 to initiate reduction processes that yield CO[133] or methoxy-boranes/methanol,[62–65] using intermolecular Zn/P and intra-molecular B/P FLPs, respectively. More related to the present review, Wen *et al.* used in 2013 DFT to investigate the hydrogenation of CO_2 by [TMPH][HB(C_6F_5)$_3$], the H_2-activated product by the TMP/B(C_6F_5)$_3$ FLP, (TMP = 2,2,6,6-tetramethyl-piperidine).[134] The H^+/H^- transfers from [TMPH][HB(C_6F_5)$_3$] to CO_2 were found to proceed in a concerted fashion through a single TS. A formic acid molecule is formed, which is subsequently deprotonated by TMP to yield [TMPH][HC(O)OB(C_6F_5)$_3$], where the formate group is bound to the B center through an oxygen atom.

At this point, computations had already granted atomically-resolved mechanistic details of both elementary steps underlying CO_2 hydrogenation (i.e. H_2 splitting and H^-/H^+ transfer). However, it was not until 2015 that Fontaine, Stephan and co-workers combined them both to study the overall hydrogenation mechanism of CO_2 with H_2 catalyzed by the intramolecular B/N FLPs, 1-BR_2-2-NMe_2-C_6H_4 (R = 2,4,6-$Me_3C_6H_2$ and 2,4,5- $Me_3C_6H_2$), as represented in Fig. 18a.[32] These FLPs were experimentally found to afford the formation of boron-bound formates, acetals and methoxides, the product ratio being sensitive to the experimental conditions of H_2/CO_2 pressures. Traces of methane were also detected at low CO_2 pressure.

The authors then applied DFT calculations to investigate the initial hydrogenation steps.[32] They include the hydrogenation of the bare FLP, followed by the formation of formic acid via concomitant H^- and H^+ transfers to an incoming CO_2 molecule. In line with previous calculations by Zimmerman *et al.*[135] and Wen *et al.*, [134] the hydrogen transfer step was found to take place with a concerted TS. Thereby, the B-bound hydride is transferred to the electrophilic C atom of CO_2, while one of the oxygen atoms of CO_2 abstracts the acidic proton from the N center of the FLP. Interestingly, the analyzed FLPs (Fig. 18a) were observed to undergo protodeborylation after H_2 splitting (Fig. 19a), giving access to 1-BHR-2-NMe_2-C_6H_4 compounds. After a second H_2 splitting step, the latter led to hydrogenated species analogous to that represented in Fig. 19b, which were found to hydrogenate CO_2 through affordable free-energy barriers. Fig. 19b shows a representative TS structure for CO_2 hydrogenation.[32]

In 2018, Jiang *et al.* studied computationally the hydrogenation of CO_2 promoted by a series of B/P intramolecular FLPs represented in Fig. 18b-d.[136] In addition to the previously established mechanism (H_2 splitting followed by the concerted H^-/H^+ transfer to CO_2, see path (i), green arrows in Fig. 20), the authors explored a novel mechanism that starts with the activation of CO_2 on the bare FLP (path (ii), purple arrows in Fig. 20). Then, metathesis of H_2 with the LB-C bond leads to an intermediate bearing an LA-bound formate and a protonated LB center, which further evolves to release formic acid regenerating the FLP. In most cases, path (i) was claimed to be more favorable than path (ii), except for FLPs shown in Fig. 18b, structures ***i*** and ***iv***. Despite the possible contribution of the mechanism associated with path (ii) (Fig. 20), path (i) which involves sequential H_2 splitting followed by hydride/proton transfer to CO_2 has been consistently adopted in subsequent computational studies on FLP-catalyzed CO_2 hydrogenation, including both

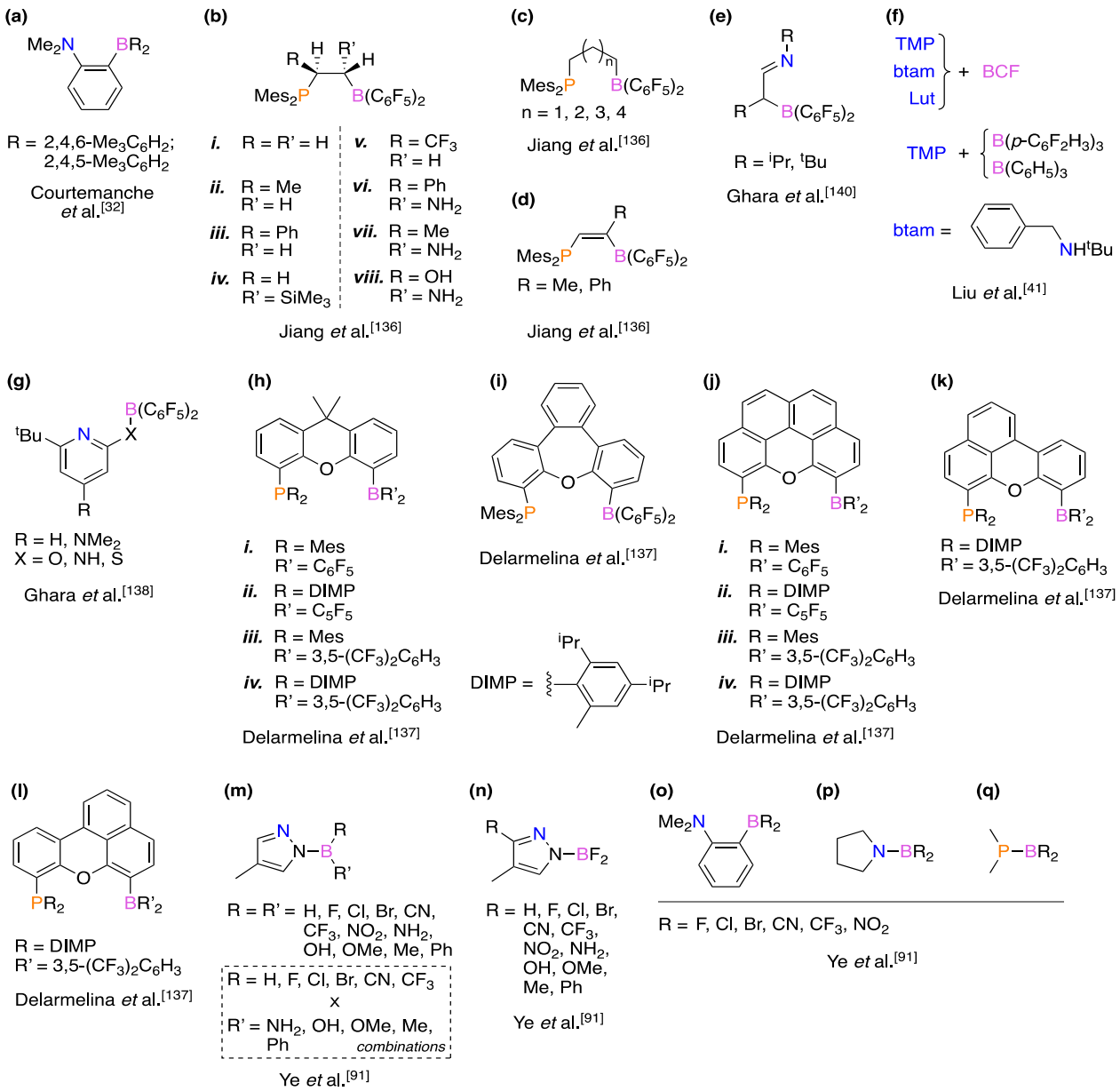

Fig. 18 Compilation of computationally studied FLP structures for CO_2 hydrogenation with H_2.

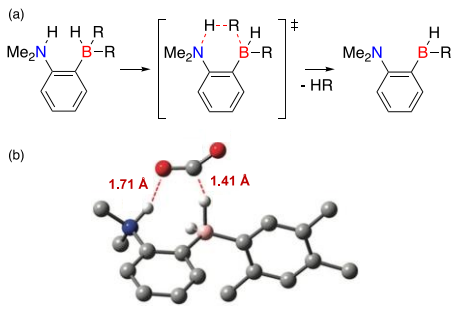

Fig. 19 a) First protodeborylation process in hydrogenated forms of 1-BRH_2-2-$NHMe_2$-C_6H_4 (R = 2,4,6-$Me_3C_6H_2$ and 2,4,5- $Me_3C_6H_2$). b) Optimized geometry of the TS for CO_2 hydrogenation by 1-BH_2(2,4,5- $Me_3C_6H_2$)-2-$NHMe_2$-C_6H_4, obtained at the ωB97X-D/6-31++G(d,p) level of theory, including benzene as solvent through the SMD continuum solvent model. Adapted from ref 32. Copyright 2015, Royal Society of Chemistry.

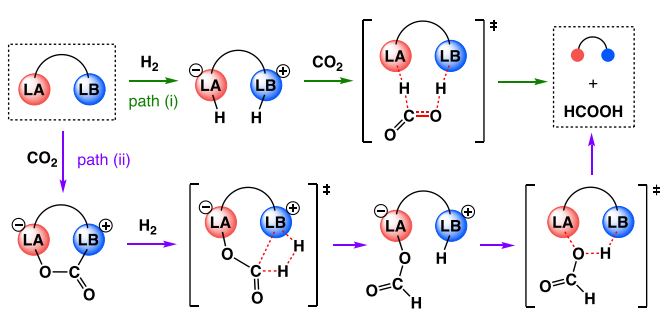

Fig. 20 Proposed pathways for CO_2 hydrogenation with intramolecular P/B FLPs.

Fig. 18e, Ghara and Chattaraj explored alternative mechanisms whereby both H_2 and CO_2 are concomitantly activated by the FLP sites.[138,140] However, these were found to involve rather high free-energy barriers, ranging from 37 to 50 kcal mol^{-1}. Besides, since the formation of non-covalent FLP···H_2 and FLP···CO_2 adducts is generally endergonic, the trimolecular nature of the proposed TSs is expected to make them kinetically unlikely. Such features render these concerted $H_2 + CO_2$ activation mechanisms not able to compete with stepwise processes represented in Fig. 20, path (i), as later proved by the same authors.[138]

3.2.2. Impact of FLP's structure on CO_2 hydrogenation activity

Understanding how the chemical structure of FLPs influences their ability to hydrogenate CO_2 is certainly more complex than rationalizing their H_2 splitting performance. This is due to the intrinsic step-wise nature of the CO_2 hydrogenation mechanism, as described in the previous section, which requires fine-tuning of the FLPs' structure to simultaneously optimize its performance for two distinct processes, i.e. H_2 splitting and H^+/H^- transfer to CO_2. This sub-section outlines the computational efforts that have been devoted so far to establishing relationships between FLPs' features and their ability to promote CO_2 hydrogenation. Note that most of the knowledge gained so far holds for FLPs that operate through path i) (Fig. 20). Conversely, path ii) (Fig. 20) has been only studied for a very limited number of FLPs and hence not enough data is available yet to attempt the development of design rules to promote this pathway.

In 2016, Liu *et al.* carried out a computational investigation aimed at finding relationships between the electronic structure of FLPs and the kinetics of CO_2 hydrogenation into formic acid.[41] In particular, their work begs important and timely questions. Is there any balance or relationship between the H_2 splitting and the hydride/proton transfer to CO_2 steps? Would a stronger FLP combination favor both steps or exclusively the H_2 splitting step as detailed above, thus being detrimental to the kinetics of the hydride/proton transfer step? Seeking to answer these questions, the authors carried out DFT calculations to analyze the free-energy profiles for CO_2 hydrogenation by five intermolecular B/N FLPs, based on combinations of $B(C_6F_5)_3$ and $B(p\text{-}C_6F_2F_3)_3$ LAs with TMP, btam and Lut LBs (see Fig. 18f). In line with the conclusions inferred from section 3.1, the kinetic analysis of the H_2 splitting step indicates that the stronger the base or the acid, the lower the free-energy barrier. However, no systematic trend was found between the FLP strength and the barriers for hydride/proton transfer for CO_2 hydrogenation. Still, stronger FLPs generally exhibit higher energy barriers for the hydride/proton transfer step assorted with later TS, thus following the opposite trend than that of the H_2 splitting step. This was ascribed to the fact that stronger FLPs are more prone to "catch and hold" protons and hydrides, hampering in turn the subsequent hydrogenation of CO_2. Later on, this phenomenon was further rationalized based on natural bond orbital and molecular electrostatic potential analyses as well as methods that are based on the application of electron localization functions.[139] In short, these showed that lower occupancies of the p(B) orbital result in stronger donor-acceptor interactions upon H_2 dissociation, thus easing H_2 splitting but hampering CO_2 hydrogenation. From a fundamental perspective, this can be interpreted as a strong (weak) Lewis base yields a weak (strong) Brønsted acid after H_2 splitting. Similarly, a strong (weak) Lewis acid partner will provide a weak(strong) hydride donor. It is apparent that the factors favouring H_2 splitting (strong LA and/or LB) might hinder the H^+/H^- transfer to CO_2.

The results described above paved the way for setting structure-activity relationships. Optimal FLPs for CO_2 hydrogenation *must balance* their ability to split H_2 with that of transferring a hydride and a proton from the zwitterionic LB^+H/LA^-H intermediate to CO_2, leading to a scenario where both steps take place through accessible free-energy barriers.Otherwise, too weak or too strong FLPs could suffer from too slow kinetics for H_2 splitting (Fig. 21, purple arrow) or hydride/proton transfer to CO_2 (Fig. 21, red arrow), respectively.

Fig. 21 Schematic free-energy profile for the two-step hydrogenation of CO_2 catalyzed by FLPs. The green profile illustrates an optimal situation where both H_2 splitting are kinetically accessible. Conversely, grey-dashed profiles represent sub-optimal situations limited either by a slow H_2 splitting step, for which the barrier is highlighted with a purple arrow; or by a slow hydride/proton transfer step, in which the associated barrier is highlighted with a red arrow.

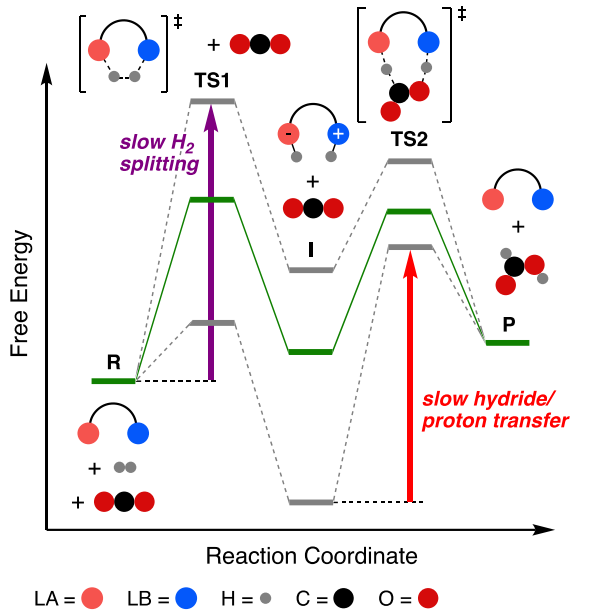

Corminbœuf and co-workers recently made substantial achievements in this context. In 2022, they reported a comprehensive computational exploration of intermolecular B/N and B/P FLPs for CO_2 hydrogenation into formate.[51] A wide spectrum of chemical space was covered with a library of 60 N- and P-based LBs and 64 triaryl borane LAs partners (Fig. 22a). Upon mutual combinations, a total of 3840 FLP candidates were computationally screened for CO_2 hydrogenation. The relative stabilities of the intermediates and TSs shown in the catalytic cycle of Fig. 22b were computed, considering the LA in catalytic concentrations and LB in excess to provide the driving force for product formation. From the above data set, two sub-pools were extracted fixing one of the Lewis partners and varying the complementary one. These sub-sets allowed exploring the individual impact of the properties of both Lewis partners. To this end, linear free-energy scaling relationships (LFESRs) were established to map the performance of the FLP on CO_2 hydrogenation as a function of two chemical descriptors, i.e. the free energy of proton attachment (FEPA) to the LBs, and the free energy of hydride attachment (FEHA) to the LAs, which were estimated as

the free energies of the following reactions (eq. 2 and 3, respectively):

$$LB + NH_4^+ \rightarrow [LBH]^+ + NH_3 \; ; \Delta G_r = FEPA \qquad (2)$$

$$LA + H^- \rightarrow [LAH]^- \; ; \Delta G_r = FEHA \qquad (3)$$

FEHA and FEPA can be regarded as direct measures of the acid and base strength of the Lewis partners, successfully employed as descriptors in the field of FLP-promoted H_2 splitting (see section 3.1). DFT-derived turnover frequencies (TOFs) were calculated as the free energy difference between the turnover-determining intermediate (TDI) and the turnover-determining transition state (TDTS) and used as a response variable that accounts for the FLPs' catalytic activity towards CO_2 hydrogenation.

Analysis of the LFESRs over the two sub-sets defined in Fig. 22a yielded volcano plots relating the FEHA and FEPA descriptors to the calculated TOFs. These plots allowed the identification of different regions as a function of the nature of the rate-determining step as illustrated in Fig. 23.b (i.e. the TDI/TDTS combination designating the TOF). On the one hand, using the rather weak B-Me_4 LA partner, most of the screened FLPs face difficulties in splitting H_2 through TS1 as defined in Fig. 22b. Strong amidine bases like DBU provide the optimal kinetic balance among the steps of the cycle, making this combination the most active. Still, the screening of the LAs using the weak pyridine LB as fixed partner revealed an over-stabilization of the boroformate complex 5 (as defined in Fig. 22b) when strong LAs with electron-withdrawing substituents are employed. Such over-stabilization is due to too strong B-O interactions. This adds energy penalty for splitting H_2 reflected in the 5/TS1 identity of the TDS/TDTS combination, as the dissociation of 5 to regenerate the bare FLP is an uphill process.

Graphing both descriptors, FEHA and FEPA, against the calculated TOF revealed a dark-red colored region where the CO_2 hydrogenation activity is maximized (Fig. 23a). Suboptimal perform-

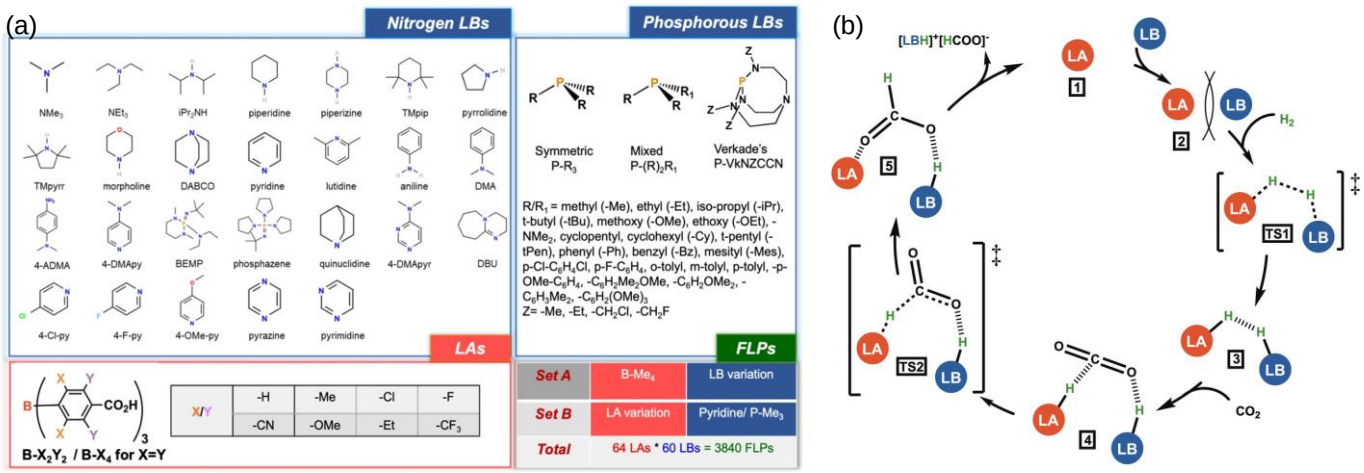

Fig. 22 a) Library of B-based LAs and N- and P-based LBs used to create a pool of intermolecular FLPs, whose potential for CO_2 hydrogenation was computationally explored by Corminbœuf and co-workers. b) Catalytic cycle considered for the generation of DFT-derived TOFs. Reprinted with permission from ref 51. Copyright 2022, Wiley-VCH GmbH.

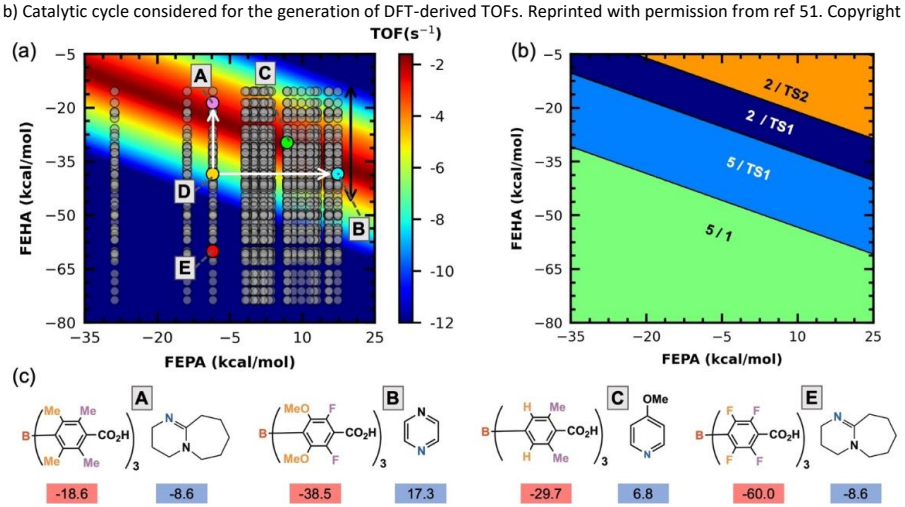

Fig. 23 a) Map correlating the TOF (log scale) for CO_2 hydrogenation into formate to FEPA and FEHA descriptors for the 1664 B/N intermolecular FLPs. b) Map analogous to that in panel (a) in which each grid point is coloured according to the identity of the TDI and TDTS. c) Chemical compositions of the FLP combinations (A–C). Their corresponding FEPA and FEHA descriptor values are shown below. D corresponds to a "mismatched combination" between the LB from A and LA from B. E is a poorly active combination with strong LA and LB components. Reprinted with permission from ref 51. Copyright 2022, Wiley-VCH.

-ances in going from red to blue-colored regions arise either from over stabilization of intermediate 5 or from high-energy lying TSs, as shown in Fig. 23b. Importantly, this work revealed that the acidity and basicity of the components have to be appropriately balanced to attain efficient FLPs for CO_2 hydrogenation, creating unprecedented mapping of FLPs chemical composition and linear scaling relationships.[51]

In the sub-field of intramolecular FLPs, the nature of the molecular scaffold or backbone that supports both LA and LB centers is an additional parameter that affects the energetics of CO_2 hydrogenation. This does not only influence the electronic properties of FLP partners but also determines their interatomic distance, allowing for strategic control of the geometrical features of the FLP pocket, which have been demonstrated to govern its reactivity.[68,129]

Using a series of intramolecular "bridged" B/P FLPs (Fig. 18b-d), Jiang *et al.* investigated how the length and the chemical nature of the bridge between P and B centers influence their CO_2 hydrogenation reactivity.[136] For alkyl-bridged FLPs, decreasing the electron-donating nature of groups in the R' position (near the B center) was found to significantly favor H_2 splitting. Still, this goes along with the formation of too stable zwitterionic intermediates that hinder hydride/proton transfer kinetics for CO_2 hydrogenation. Similarly, for intramolecular B/N FLPs shown in Fig. 18g, Ghara *et al.* [138] reported that the free-energy barrier for H_2 splitting decreases upon the incorporation of an amino group in the para position of the pyridine ring, while the barriers also decrease in the order X = NH > O > S. However, S-containing systems have more difficulties than the others in reducing CO_2. Elongating the bridge length in intramolecular B/P FLPs (Fig. 18c) was found to have a detrimental impact on CO_2 hydrogenation, as Jiang *et al.* reported a systematic increase of the barriers for both H_2 splitting and CO_2 hydrogenation steps due to an increase of the strain in the TSs. [136] Vinyl bridges (Fig. 18d**)**, were not identified as promising candidates neither because they yield very stable zwitterionic intermediates after H_2 splitting, hindering hydride/proton transfer steps.[136]

The flexibility of the backbone, which impacts LA···LB separation, has been also identified as a relevant parameter to tune the reactivity of intramolecular B/P FLPs towards H_2 and CO_2 to produce formic acid.[137] Inspired by the application of dimethylxanthene backbones to prevent the self-quenching of the FLP components,[141] Delarmelina *et al.* analyzed in detail a series of xanthene-inspired scaffolds which display various P···B distances (Fig. 18h-l, Fig**.** 24). Compound **H** (Fig**.** 24) is found active for H_2 splitting in line with experimental observations,[141] but exhibits a very height barrier for the CO_2 hydrogenation step. Compared to **H**, both compounds **I** and **J** (Fig**.** 24) show slightly higher but still affordable barriers for H_2 splitting. However, the impact of their backbone on their CO_2 hydrogenation step was found to be very different: Catalyst **I**, which displays a shorter P···B distance than **J**, has a very high barrier for the second step; conversely, in **J,** the more rigid backbone and longer P···B distance led to a substantial decrease of the free-energy barrier for hydride/proton transfer to CO_2 when compared to **H** and **I**, which translates into a reduction in the activation energy for the whole process. Further tuning of the FLPs **H**-**J** via modification of the electronic properties of the substituents at the B and P groups was found to play a secondary role compared to the stiffness of the backbone. Of note, Delarmelina *et al.* also reported that more polar solvents stabilize both the zwitterionic intermediate and the TS of the second step. Still, such stabilization is very similar in both cases, having an overall negligible impact on the height of the CO_2 hydrogenation barrier.[137]

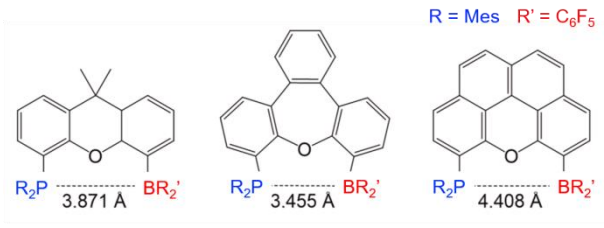

Fig. 24 P···B interatomic distances (Å) between P- and B-centers of FLPs **H**, **I** and **J** studied computationally by Delarmelina *et al.*[137] Adapted with permission from ref. 137. Copyright 2021, Elsevier.

3.2.3. Computational analysis of potential poisoning and inhibition routes.

As described in the previous section, CO_2 hydrogenation is commonly assumed to require a perfectly orchestrated sequence of H_2 splitting followed by hydride/proton transfer to a CO_2 molecule to yield formic acid, regenerating the bare FLP and thus, closing the catalytic cycle. However, the topology of potential energy surfaces can sometimes favor side processes that may compromise the efficiency of the targeted process. Besides comprehensively analyzing CO_2 hydrogenation pathways and the factors that govern them, computational techniques have been also employed to identify and explore potential poisoning routes or side processes that can be detrimental to CO_2 hydrogenation.

Owing to the well-known ability of FLPs to activate CO_2-forming LB-C(O)O-LA adducts,[54,142–144] the competition between H_2 and CO_2 for the binding sites of FLPs is intrinsic to the conditions required for catalytic CO_2 hydrogenation, in which the FLPs are exposed to a mixture of both reagents. Thus, depending on the thermodynamics and kinetics of CO_2 binding, the latter may be regarded as a potential poisoning route, precluding CO_2-hydrogenation reactivity. If the formation of a covalent FLP-CO_2 complex is exergonic and faster than H_2 splitting (Fig. 25, light-blue dashed lines), the H_2 splitting process will be slowed down. This is because the overall barrier that needs to be overcome corresponds to the free-energy difference between the FLP-CO_2 complex and the TS1 for H_2 splitting, as exemplified in Fig. 25 ($\Delta G^{\ddagger}_{overall,1}$, light blue arrow). In the worst-case scenario, this can even inhibit H_2 splitting (and subsequent CO_2 hydrogenation) if CO_2 binding is irreversible or if the resulting overall barrier is too high to be overcome at the experimental conditions. Still, it should be noted that for systems that can operate through path (ii) (Fig.20) thanks to a low FLP-CO_2→TS1' barrier, the preferred binding of CO_2 with respect to H_2 splitting might not lead to a poisoning route but rather to an in-cycle species. However, the factors that determine the preference for one path or another remain elusive, making it difficult to predict whether a given FLP would be able to bypass the limitations underlying competitive CO_2 binding processes by proceeding through this alternative mechanism.

Assuming path (i) in Fig. 20 (sequential H_2 splitting followed by H^+/H^- transfer to CO_2) as the mechanism at work, computational studies aimed to identify the factors that determine the relative affinity of FLPs toward H_2 and CO_2,[91,121,145] hence providing guidance to favor H_2 over CO_2 binding. Changing the electronic properties of FLP sites via tuning of LA/LB substituents of structures shown in Fig. 18m-q was only found to either strengthen or weaken the adsorption of both H_2 and CO_2. Conversely, shortening the LA···LB distance can simultaneously strengthen the H_2 adsorption and weaken the CO_2 adsorption.[91] Also, thermodynamics of H_2 and CO_2 binding can be controlled by playing with the electron-conjugation properties of FLPs. In particular, gains in aromaticity of the FLP structure along CO_2 binding were found to result in lower activation energies and more enhanced exergonicity due to the stabilization of TS and product structures.[121] On the other hand, reduction of anti-aromaticity along H_2 splitting is also beneficial in terms of kinetics and thermodynamics.[145] Thus, although not straightforward to control, these properties may be also tapped to achieve tailored H_2/CO_2 binding selectivity.

Akin CO_2 or H_2, the formic acid product resulting from CO_2 hydrogenation can also form strong covalent adducts with bare FLPs, as illustrated in Fig. 25 (red dashed lines), which could hamper the subsequent H_2 splitting process to initiate a new cycle. One of the rare examples of computational works that considered the participation of FLP-HCOOH complexes as *in-cycle* species for CO_2 hydrogenation (Fig. 22b) revealed that these complexes act as the resting state of the catalyst in a wide range of LA/LB combinations (Fig. 23).[51] Comparable occurrences may be also expected for further reduced species such as methanol. The latter has been reported to strongly bind boron LA centers of FLPs forming B-methoxy species, both computationally[134] and experimentally.[62–65] To circumvent these issues, as well as to provide the thermodynamic driving force for the *per se* endergonic CO_2 hydrogenation reaction, bulky bases such as DBU may be used to "trap" the HCOOH product as [Hbase][HCOO] salts, while leaving unaltered LA sites of FLPs by avoiding quenching through steric repulsion (see Table 1).

Finally, as the vast majority of FLPs rely of boron LA centers, common FLPs are highly sensitive to moisture due to the oxophilicity of boron atoms. Moreover, they can also suffer from other degradation or inhibition pathways, such as protodeborylation, as shown in section 3.2.1 (Fig. 19a).[32] conspicuously, this could either promote the complete degradation of the FLP or lead to partially protodeborylated species with enhanced activity. DFT calculations suggested that the ability of FLPs to undergo protodeborylation may be modulated by tuning the steric hinderance around the B-C bonds, so that crowded environments hamper this process, allowing control over the electronic and steric properties around boron LA sites during the course of the reaction. In general, this process is commonly overlooked in the literature, although its assessment appears to be necessary to evaluate or predict the activity of an FLP towards CO_2 hydrogenation. Otherwise, FLPs that may be initially predicted to be inactive could become active upon protodeborylation and vice versa.

3.2.4. Concluding remarks.

This entire section demonstrates that achieving efficient FLP catalysts for CO_2 hydrogenation requires a delicate balance between the FLP's capability to cleave H_2 and the ability of the hydrogenated FLP to transfer a proton and a hydride to CO_2 while also preventing or minimizing potential routes of poisoning. This requires granting an appropriate CO_2/H_2 affinity towards FLP sites and allowing the FLP-HCOOH complex to liberate the product.

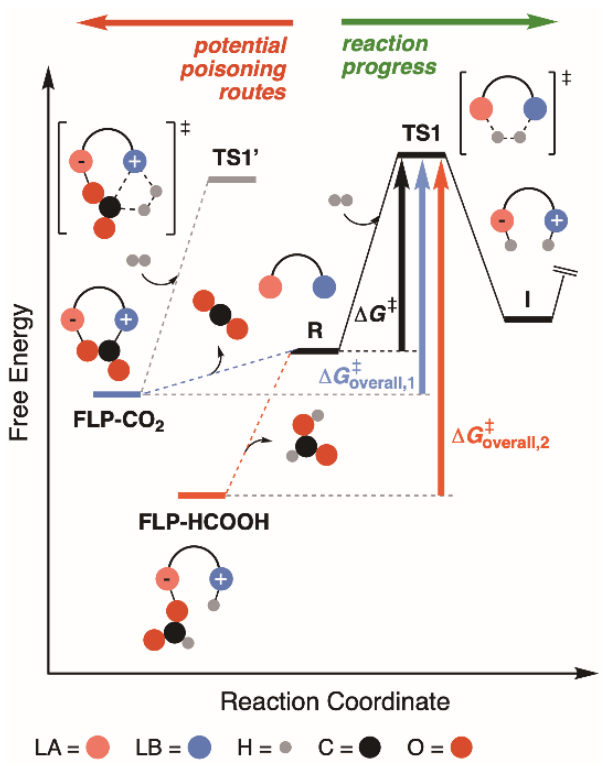

Fig. 25 Schematic free energy profile for the early steps of CO_2 hydrogenation, highlighting the impact of possible stabilizing interactions between the bare FLP and CO_2 (light-blue dashed lines) or formic acid (red dashed lines) on the kinetics of H_2 splitting. Black, light-blue and red arrows represent the individual free-energy barrier for the H_2 splitting step ($\Delta G^{\ddagger}$), and overall barriers for the same process measured from stable FLP-CO_2 ($\Delta G^{\ddagger}_{overall,1}$) and FLP-HCOOH ($\Delta G^{\ddagger}_{overall,2}$) complexes, respectively. TS1' accounts for possible hydrogenation of CO2 through path (ii) of Fig.20.

Most of the knowledge gained from the computational study of molecular FLPs may apply to the design of heterogenized FLPs inside porous matrices for the sake of avoiding the limitations inherent to homogeneous systems. However, such a heterogenization strategy poses a series of additional challenges, related to the stability of the functionalized materials, the dynamics and accessibility of FLPs within the pores of the material, the selectivity of the material towards CO_2/H_2 adsorption, or the impact of confined environments on the electronic and structural properties of FLPs, as discussed in the following section.

3.3 FLPs heterogenized into porous solids for CO_2 hydrogenation

3.3.1 Immobilizing Intramolecular FLPs in MOFs

So far, only a handful number of computational studies have considered the full immobilization of intramolecular FLPs in MOFs for CO_2 hydrogenation. In these reports, the role of the pristine MOF consists of an inert support, i.e. with no participation of either organic linkers or inorganic subunits in the reaction. The catalytic activity of the molecular FLP is thus "transferred" to the porous solid through its covalent grafting to one of the MOF's organic linkers, allowing the *in silico* evaluation of its stability and reactivity in the resulting FLP@MOF solid. So far, such studies have been mostly devoted to the Zirconium-based UiOs (University of Oslo) subfamily of MOFs.[146] Such focus on UiOs is directly related to their experimentally well-known chemical and thermal robustness and the possible post-synthetic functionalization of their organic linkers.[147]

A couple of computation studies have considered the possibility that Zr-based MOF may possess built-in frustration between LA and LB centers. Along that line, Slater *et al.* have conducted extensive ab initio molecular dynamics (AIMD) simulations on the defective Zr-based UiO-66.[148] They show that missing terephthalate linkers are charge-balanced by hydroxide anions bonded to under-coordinated Zr sites, where rapid proton shuttling may be involved with physisorbed atmospheric water molecules. At high activation temperatures, AIMD simulations further reveal that FLP sites may form consisting of an undercoordinated Zr site (Lewis acid) adjacent to a hydroxide bonded to a proximal undercoordinated Zr atom (Lewis base). The authors suggest that similar defects may exist in a wide range of MOFs, whereby increased catalytic activity and tailoring of the functional behavior could be targeted.

More recently, a detailed DFT study considered the mechanistic details of CO_2 hydrogenation to methanol in the linker-defective UiO-66, exploring various pathways and free-energy profiles on the resulting metal-based FLPs.[149] The defective model of UiO-66 is created by removing an organic carboxylate linker from a Zr6-oxocluster node, leaving behind two adjacent undercoordinated Zr sites. One of them is proposed to act as a Lewis acid, while the -OH group added to the other Zr site for charge balance purposes acts as a Lewis base. The hydrogenation consists of a three-stage transformation: i) CO_2 is hydrogenated into formic acid (HCOOH); ii) HCOOH is converted to formaldehyde (HCHO) via hydrogenation and dehydration; iii) HCHO is hydrogenated into CH_3OH. For CO_2 hydrogenation to HCOOH, three possible pathways were investigated (Fig. 26). Typically, in pathway III, H_2 is initially located above the open Zr site (LA) and the hydroxide (LB) and dissociates, leading to a Zr-H hydridic site and a vicinal Zr-H_2O water molecule. CO_2 is then hydrogenated into formic acid (FA) via a slightly endergonic concerted mechanism overcoming an energy barrier of 10.2 kcal.mol^{-1}. The cis-FA desorbs to the gas phase and then transforms into the trans-FA. HCOOH is then converted at the FLP in a stepwise fashion into formaldehyde HCHO and CH_3OH via facile H_2 dissociation and the concerted H^+/H^- transfer to HCOOH and HCHO. Interestingly, the authors explored the impact of a possible confinement effect in UiO-66 on the catalytic activity by considering two sizes (small/large) of clusters. It was found the energy barriers obtained with the two types of clusters differ only by 2 kcal mol^{-1}, suggesting that the confinement effect in UiO-66 is negligible.

Leaving apart these specific cases where the pristine MOF was studied for its intrinsic "FLP-like" catalytic properties for CO_2 reduction,[149] we are not aware of computational studies of functionalized FLP@MOF systems where the MOF itself plays a catalytic role as a Lewis partner for CO_2 conversion.

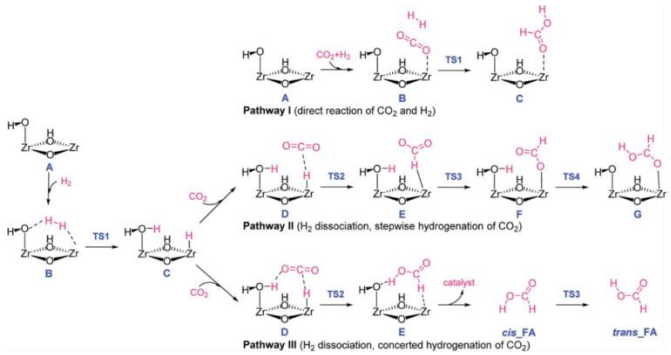

Fig. 26 Proposed pathways for CO_2 hydrogenation to HCOOH in the linker-defective UiO-66. Reprinted with permission from ref. 149 from the Royal Society of Chemistry.

Johnson and Ye pioneered the design of FLP@MOF by covalently grafting an intramolecular FLP to the terephthalate linker of UiO-66[88,89] or embedding the FLP in UiO-67[90] to study catalytic CO_2 hydrogenation mechanisms. They aimed to functionalize UiO-66 with 1-(difluoroboranyl)-4-methyl-1H-pyrazole (P-BF_2), developed to mimic 1-[bis(pentafluorophenyl)boryl]-3,5-ditert-butyl-1H-pyrazole FLP, which is known to cleave H_2 heterolytically and fixe CO_2.[150,151] The less bulky P-BF_2 was modelled by removing the tert-butyl groups and replacing C_6F_5 moieties by F atoms. Constructing the UiO-66-P-BF_2 *in silico* with one P-BF_2 group per primitive cell, static-DFT calculations in the gas phase provided relative energy profiles for CO_2 chemisorption, H_2 dissociation, and CO_2 hydrogenation to formic acid, without accounting for entropic contributions.[88] Two pathways were compared: CO_2 activation followed by H_2 cleavage or concerted H_2 cleavage and CO_2 hydrogenation. The first pathway involving the chemisorption of CO_2 in UiO-66-P-BF_2 lead to the formation of a very stable adduct and a potential poisoning of the FLP. The second pathway was found energetically more favourable than the first with a much lower activation barrier, making it the desired one. The MOF environment slightly reduced the barriers for H_2 dissociation and CO_2 hydrogenation compared to the isolated P-BF_2 catalyst, though the absence of entropic contributions suggests caution.

Expanding on their initial proof-of-concept, the authors explored UiO-66-P-BR_2 variants for CO_2 hydrogenation,[89] testing various electron-donating and -withdrawing substituents on the acidic partner while keeping the same diazole basic partner (see Fig. 17a). The process in the gas phase involved H_2 heterolytic splitting (as presented in section 3.1), CO_2 chemisorption, and concerted hydride and proton transfer to form formic acid. They again identified BEP relationships for rapid screening of functional acid groups, finding that energy barriers for CO_2 hydrogenation correlated linearly with H_2 dissociation energy in the UiO-66-P-BR_2 series (Fig. 27a). Weaker H atom bonds consistently facilitated H^-/H^+ transfers, easing CO_2

hydrogenation. H_2 splitting energies served as a first estimate for CO_2 hydrogenation barriers. A Sabatier activity map combined BEP relationships for H_2 dissociation barriers (i.e. B's hardness) and CO_2 hydrogenation barriers (i.e. H_2 dissociation energy), revealing optimal functional groups with hardness above 3.8 and H_2 binding energies between -0.45 and -0.1 eV (red area in Fig. 27b).

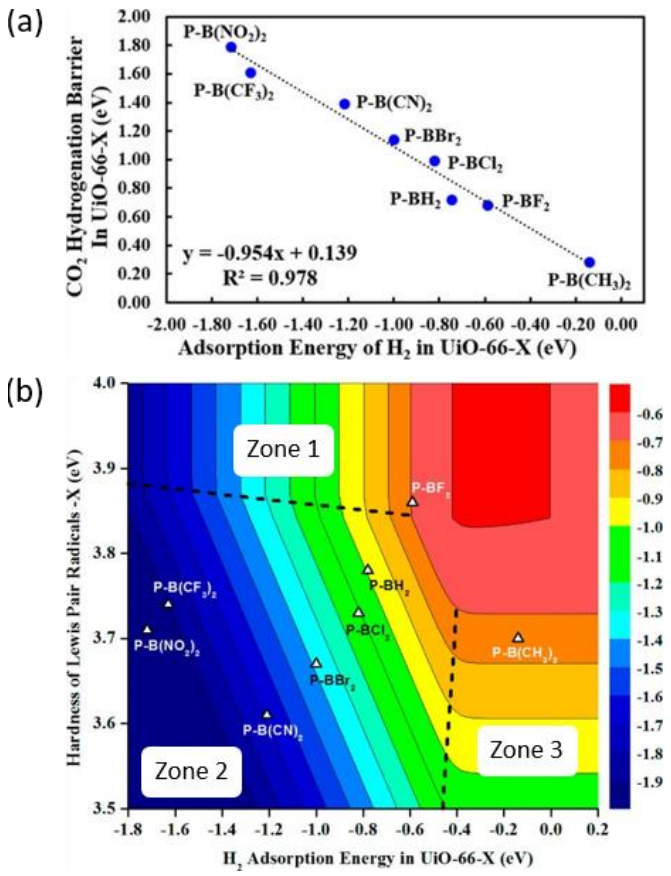

Fig. 27 (a) BEP relationship between CO_2 hydrogenation barriers and dissociation energies of H_2 in UiO-66-P-BR_2. (b) Sabatier activity map for overall CO_2 hydrogenation at 298 K. The CO_2 hydrogenation barriers are given by a BEP relationship with H_2 dissociation (adsorption) energies (x-axis) and H_2 dissociation barriers have a BEP scaling with the hardness of the LPs. Reprinted with permission from ref 89. Copyright 2015, American Chemical Society.

So far, we are not aware of any experimental report on the functionalization of UiO-66 with P-BF_2. The functionalization of this well-known MOF with FLPs is yet to be reported and may be hindered by practical synthetic limitations, discussed above in section 2.2. Notably, Johnson et al were the first to have screened the reactivity of FLPs anchored in MOF and attempted to find descriptors for their catalytic activity in CO_2 hydrogenation. Still, descriptors related to the MOF's impact as a "secondary coordination sphere" of the FLP on the CO_2 hydrogenation-free energy profile are yet to be identified.

Along this line, the same authors have compared the impact of pore size and topologies of MOFs on the dissociation of H_2, the chemisorption of CO_2 and its reduction into formate, examining MOFs with increasing pore sizes: MIL-140B (~8 Å) < UiO-66 (~5 Å and ~9 Å) < MIL-140C (~10 Å) < UiO-67 (~12 Å and ~16 Å).[92] The Lewis pairs are comprised of N and BF_2 moieties linked via a C atom, embedded in the organic linker, except UiO-67 where the LP is part of a side chain pointing towards the pore center, generating minimal steric interaction with the hosting framework. The calculated dissociation energies of H_2 are found similar in all systems, suggesting that pore size and confinement effects have no significant impact because of the small size of H_2. In contrast, CO_2 chemisorption energies exhibit significant differences among the four MOFs. They depend on the orientation of the bound CO_2 and the proximity of carboxylate O atoms of nearby linkers, which may result in strong repulsions with CO_2. The strongest chemisorption of CO_2 observed in UiO-66-P-BF_2 is allowed by the minimal steric interactions between the LP and this MOF. By contrast, the lower strengths of CO_2 chemisorption in the three other systems are a subtle convolution of the flexibility of the MOF's linker and specific confinement effects around CO_2 imposed by the number of linkers per secondary building units. Turning to the CO_2 hydrogenation process, the authors claim that confinement and steric hindrance may allow the selection of specific MOF topologies to i) favor the dissociation of H_2 over the chemisorption of CO_2, thus increasing the resistance of the MOF to CO_2 poisoning, and ii) improve the catalytic performances by pre-activating CO_2 via a bent physisorbed configuration.

Johnson *et al.* also considered UiO-67 (Fig. 28a) - due to its larger pore volume and surface area than that of the isostructural UiO-66 - for hosting an intramolecular FLP, namely UiO-67-$(NBF_2)_4$ (Fig. 28b).[90] Notably, the adsorption energy of CO_2 was found to be much lower than that of H_2 (-0.22 eV versus -0.50 eV). This allows a much easier desorption of chemisorbed CO_2 and avoids the poisoning of the FLP by CO_2 that was previously observed in UiO-66-P-BF_2. Overall, UiO-67-$(NBF_2)_4$ provides multiple LP catalytic sites for H_2 dissociation, making facile reduction of CO_2 to methanol possible without requiring diffusion of the intermediate reactants or products into adjacent pores. The reaction pathways to methanol involve a series of concerted two-hydrogen transfer steps where the following pathway, CO_2 → cis-HCOOH → $CH_2(OH)_2$ → CH_2O → CH_3O_H, has the lowest potential energy surface, HCOOH acting as a proton shuttle.

Heshmat reinvestigated in depth the above UiO-66-P-BF_2 catalyst using ab initio molecular dynamics (AIMD) simulations, computing free energy surfaces (FESs) using metadynamics.[93] Here, the thermal and entropic contributions to the free energy profile were taken into account thanks to the motion of H_2/CO_2 molecules in the gas phase within the LP-functionalized MOF. The mechanism of CO_2 hydrogenation towards formate was shown to be more eventful than initially proposed by Johnson *et al.*,[89] with the possibility of a stepwise mechanism in addition to the concerted one, while providing unique features about the dynamics of the reaction.

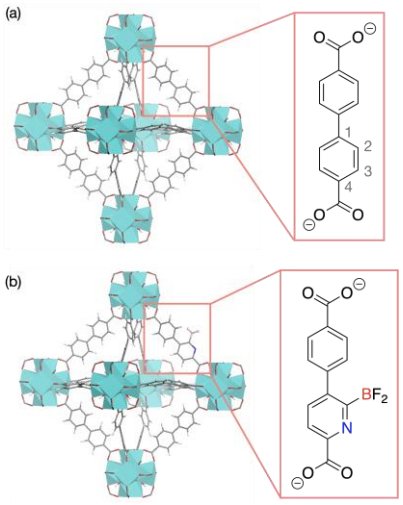

Fig. 28 (a) Representation of the native UiO-67 and its biphenyl linker and (b) the modified UiO-67 incorporating a ligand with a B/N intramolecular FLP.

The free-energy barrier for H_2 splitting was found to be affordable (18.8 kcal mol^{-1}), being ca. 6 kcal mol^{-1} higher than the reported electronic energy barrier reported in Johnson's work,[89] due to the incorporation of entropic effects. Also, simulations revealed that the formation of the zwitterionic intermediate (hydrogenated FLP) is thermodynamically favorable by ca. 6 kcal mol^{-1}. Importantly, although the free-energy barrier for CO_2 activation by the bare FLP was estimated to be 10 kcal mol^{-1}, being lower than that for H_2 splitting, the reverse free-energy barrier for CO_2 desorption was computed to be affordable as well, accounting for 21.1 kcal mol^{-1}.[93] This suggests that even though CO_2 binds stronger to the FLP than H_2, the formation of FLP-CO_2 adducts does not necessarily imply poisoning of the catalyst. Still, in the presence of a CO_2/H_2 mixture, H_2 splitting would be precluded by an overall free-energy barrier of close to 30 kcal mol^{-1} (H_2 splitting barrier + energy span associated to CO_2 desorption from the FLP). On these grounds, it is postulated that suitable CO_2 hydrogenation conditions might involve exposing the MOF sequentially to separate streams of H_2 (to activate it on the FLP) and CO_2 (to hydrogenate it), rather than to a mixture of CO_2 and H_2, whereby the binding of CO_2 to FLP sites would hamper H_2 splitting.

The FESs for the next CO_2 hydrogenation step were calculated using *cis* and *trans* conformations of dissociated H_2. The *cis* conformation reveals an asynchronous concerted mechanism, while the *trans* conformation shows a stepwise mechanism with H^- is transferred to C(CO_2) first, followed by H^+ to O(CO_2) after 400 fs. Both mechanisms are kinetically feasible and endergonic. The hydrogenation of CO_2 may be thus fully described using the two $H^-\cdots B$ and $H^-\cdots C(CO_2)$ distances as collective variables. Atomic charges analysis indicates a more polarized B-H bond vs the N-H one, causing an earlier hydride than proton donation. This is also reflected in the 1 eV higher HOMO-LUMO energy gap between the lone pair of O(CO_2) and N-H σ^* than that between the B-H σ orbital and π^* of activated CO_2. MD simulations reveal strong interactions between the HCOOH product and Zr-clusters of the MOF, in line with known observations in Zr-based MOFs,[152] implying the need for continuous HCOOH removal for high conversion rates.

Another recent computational study investigated the Zr-based UiO-66 MOF functionalized with alanine boronic acid for CO_2 hydrogenation.[153] The energy profile for CO_2 hydrogenation in the gas phase of the immobilized FLP in UiO-66 is compared to that of the isolated molecular FLP. These calculations suggested an overall stabilization along the whole energy profile as the reaction proceeds in the FLP@UiO-66 solid, although entropic contributions were not considered. A notable decrease of 4.6 kcal mol^{-1} in the H_2 splitting barrier was estimated upon immobilization of the FLP. Also, the comparison of the various components of the energy decomposition analysis (EDA)[154] (electrostatic, Pauli repulsion, dispersion and orbital interactions) reveals a greater stabilization of reaction intermediates and transition states in the FLP@MOF system when compared to that obtained with the isolated FLP, pointing towards a beneficial impact of the confinement of the reaction within the MOF's pores.

3.3.2 Impact of immobilizing intermolecular FLPs on catalytic activities

The previous section focused on the targeted immobilization of a single intramolecular FLP into a porous inert host. Immobilizing both LA and LB partners as independent molecular species within the pores or channels of a MOF poses a more challenging target. This requires functionalizing the host with two chemically distinct species instead of just one. Still, it might be considered as a more attractive approach than the immobilization of a single intramolecular FLP for several reasons. Firstly, the successful anchorage of both the Lewis acids (LA) and Lewis bases (LB) to the MOF could be used to prevent the quenching of their reactivity. Secondly, the separate anchorage of the LA and LB partners at distinct positions of the MOF opens - in theory - the possibility of controlling the LA···LB distance, which may not be attainable in homogeneous conditions. Lastly, such strategy significantly increases the number of possible LA/LB combinations to explore when compared to those accessible in homogeneous conditions, thanks to the prevention of quenching.

However, there are key issues that need to be addressed in order to fully benefit from the aforementioned advantages of the immobilization of intermolecular FLPs. Firstly, it is crucial to control the synthetic or post-synthetic modifications of the MOF to achieve the desired relative positioning of the LA and LB centers within the required distance. Secondly, it is required to preserve the steric accessibility and chemical environment of both the LA and LB partners once anchored, in order to avoid any detrimental interactions between the LA or LB partners and the MOF. This raises yet-to-be-answered questions regarding the dynamics of both the MOF and the LA/LB partners. Lastly, it requires identifying the most suitable MOF structures from the vast number of existing ones that can meet the aforementioned constraints, while also considering the practical issues related to the compatibility of their synthesis protocols, thermal and chemical stability with those of the FLPs to be immobilized. In that respect, computational chemistry approaches have a key role to play, not only for exploring the potential catalytic performances of LA···LB pairs once immobilized within the MOF, but also for predicting the overall impact of their immobilization in the MOF pores or channels. The latter includes considerations on LA and

LB's spatial partitioning, steric, chemical or electronic features and dynamical behavior within the MOF, to ultimately identify design principles.

In that direction, Corminbœuf *et al.* explored the constrained spatial arrangements of the prototypical BF_3/pyridine Lewis pair.[68] Using the B···N distance (*d*) and the angle (*Φ*) formed by the B's empty orbital and the N's lone pair as descriptors, the complete free energy profile for CO_2 hydrogenation for intermediates and transition states as defined in Fig. 22b was evaluated at each increment of the B···N distance (0.1 Å steps), while allowing *Φ* to adapt freely (Fig. 29a). Fitting it to a Morse potential, a scaling relationship was created that predicts the reaction's rate or TOF (turn over frequency) based solely on the B···N distance. This allowed them to estimate the resulting gain or loss of catalytic performance of the « immobilized » FLP to the unconstrained one (ΔTOF), thus providing direct insight into how restricting the FLP's geometry affects its activity. The complete activity profile was constructed as depicted in Fig. 29b.

Remarkably, these calculations reveal that the catalytic activity of an N/B FLP may be boosted by constraining its geometry. The peak performance (dark red area in Fig. 29b) is estimated to be eleven orders of magnitude higher than that of the unconstrained FLP (ΔTOF = 0). High efficiency can be achieved over a wide range of distances as long as the N···B orientation is suitable. The optimal orientation for H_2 activation is in the range of *Φ*=90°-135°, which suggests that promoting this step through immobilization could enhance the catalyst's efficiency. Notably, the predictive capability of the activity map was successfully validated against reported intramolecular N/B FLPs and known experimental trends from Fontaine *et al.* on amine-boranes[32] for CO_2 hydrogenation.

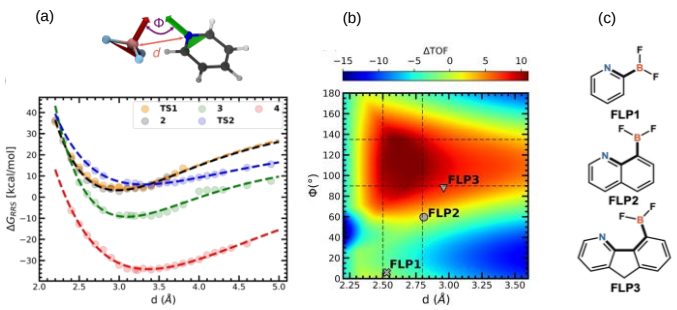

Fig. 29 FLP-catalyzed hydrogenation of CO_2 following the catalytic cycle described in Fig 31b. (a) Energy-distance scaling relationship showing the variation of free-energies of each intermediate and transition state with the *d* descriptor (*d* = LA…LB separation in Å), fitted with Morse potentials (dashed lines); (b) Activity map describing the relative TOF of constrained FLPs with respect to unconstrained FLPs as a function of the key descriptors, *d* and Φ; (c) Intramolecular FLPs that are mapped in (b) and the geometric descriptor values extracted from the corresponding intermediate **2**. Copyright 2022 from ref 68. Angewandte Chemie International Edition published by Wiley-VCH GmbH under the terms of the Creative Commons license.

This pioneering work of Courminbœuf *et al.* presents a comprehensive and generic conceptual approach to immobilizing FLPs in any type of solid-state system, regardless of structure and chemical environment of the host, as the explored geometric constraints closely resemble those that arise from FLP's immobilization. Although the specific influence of the host on the FLPs' chemistry is not addressed, these findings convincingly demonstrate that constrained geometry correlates with a distinct catalytic activity. The strategic confinement of the FLP within specific distances and orientations can unexpectedly trigger enhanced catalytic activity compared to the unconstrained FLP. Overall, this proposed approach has the potential to inspire future investigations for screening the catalytic activities of other chemical LA-LB partners in CO_2 hydrogenation and identifying optimal constrained geometries to be further incorporated into MOFs or porous polymers for instance.

4. Lessons learned from experimental and computational studies

With tremendous achievements in both the experimental discovery of main group elements FLP systems and the computational understanding of their reactivity, the careful analysis of these two prolific sides of such a subtle chemistry opens opportunities for installing a dialogue between experiments and calculations, exemplified for the CO_2 hydrogenation reaction.

4.1 Finding the sweet spot of reactivity with H_2 and CO_2

H_2 splitting and CO_2 hydrogenation processes generally follow opposite trends with variations of most of the FLPs' properties, whereby whatever favors one is detrimental to the other. It is thus inevitable to outline parallelisms with the Sabatier principle, widely used in heterogeneous catalysis to describe an optimal catalyst that binds substrate molecules strong enough to enable reactivity but not too much to prevent undesired poisoning issues. Hence, pinpointing optimal FLP catalysts for CO_2 hydrogenation with H_2 demands the identification of *sweet spots* that balance the feasibility of both H_2 splitting and subsequent CO_2 hydrogenation step.

In this regard, the development of computationally driven strategies to identify sweet spots where the energetics of both steps are balanced to achieve optimal CO_2 hydrogenation activity represents a matter of current research, and some guidance and rules of thumb have been recently reported. Specifically, optimal CO_2 hydrogenation activity has been found to require a *moderate* cumulative acid/base strength, which can be estimated as the sum of proton and hydride attachment energies to the LA/LB partners (FEPA and FEHA, respectively). Thus far, systematic explorations have been only carried out with intermolecular B/N FLPs, which revealed that the TOF is maximized for LA/LB combinations with FEPA/FEHA ratios ranging linearly from ca. -35/-10 to +25/-35 kcal mol^{-1}.[51] Moving away from these ranges leads to too strong pairs, which form too stable zwitterionic hydrogenated FLP intermediates or bind products too strongly, or to too weak pairs, which have difficulties splitting H_2.

Also, intramolecular FLPs allow for some "tricks" to move orthogonally away from these trends, by controlling either the LA···LB distances or the rigidity of the molecular scaffolds, as exemplified by the work by Delarmelina *et al.*[137] More rigid backbones and longer LA···LB distances (of ~4.4 Å) was found to substantially reduce the free-energy barrier for hydride/proton transfer to CO_2, compared to more flexible scaffolds with LA···LB distances of < 4 Å. While for H_2 splitting, optimal B···N distances were found to lie in a range of 2.6–3.5 Å,[68] not a single study has claimed

yet what is exactly the optimal LA···LB distance to promote CO_2 hydrogenation and how it varies as function of the nature of the FLP sites. Still, it is reasonable to assume that optimal performances would be found at the overlap of distance ranges that are suitable for both H_2 splitting and H^+/H^- transfer elementary steps.

In addition, potential poisoning pathways such as competitive binding of species on FLP sites or protodeborylation, are analyzed independently in the literature, but rarely (if ever) in a joint manner to grant a full mechanistic picture of the reaction. Regarding the latter routes, some trends have been found for specific sets of FLPs. These include: shortening of LA···LB distances to favor the activation of H_2 by FLPs over that of CO_2; or increasing the steric hinderance around B sites to prevent undesired protodeborylation events.

Moreover, beyond the determination of the adequate energetics balance and the inclusion of poisoning in computational approaches, the calculated data should be translated into experimental parameters such as partial gas pressure and temperature, which remain crucial towards applicable CO_2 hydrogenation systems. For instance, a pioneering system by Corminbœuf and Dyson allows for the FLP-driven CO_2 reduction at 120°C under 130 bars, specific conditions that were not anticipated from the calculated data but must have required intensive experimental screening.[51]

4.2 Challenges in turning computational chemistry into target synthesis

Recently, computational chemistry approaches have become an extremely powerful tool for screening the potential use of molecular FLPs for CO_2 hydrogenation, identifying successful LA-LB pairs, which were later verified experimentally. Still, the translation of computational learning into the experimental realm remains far from trivial, especially when tackling the challenge of FLPs' heterogenization.

Two experimental aspects have to be considered when turning computational results into bench-scale trials: the synthetic accessibility of the FLP synthons and the conditions to be applied to reach the targeted FLP's reactivity. Considering the reactivity of computationally designed FLPs for the CO_2 hydrogenation, the conditions reported in the two recent examples by Zhao[50] and Corminbœuf,[51] both claiming for a catalytic FLP system, were 160°C under 60 bars of CO_2/H_2 and 120°C under 130 bars, respectively. Far from being trivial, the findings of such harsh conditions to assess the efficiency of carefully designed Lewis pairs can only rely on a large screening of pressures and temperatures, including a range of values not often investigated for molecular catalysis. Thus, the quest for novel experimental FLP systems for CO_2 hydrogenation, whether predicted by preliminary computational studies or not, must encompass from its beginnings these specific ranges of temperatures and pressures, especially when compared to transition-metal-based counterpart systems operating under smoother conditions. [155]

Besides the deployment of dedicated organic synthesis of the predicted FLPs, limitations that are related to their heterogenization may emanate from the reactivity/stability of the porous solids (MOF, POP, COF) themselves upon their functionalization with the targeted FLPs. Additional drastic limitations may arise from the catalytic conditions themselves (pressure, temperature, solvent…). In the proposed two-step synthetic pathway devised by Ye and Johnson[90] for targeting the MOF-heterogenized FLP UiO-67-P-BF_2, the initial step hinges upon a palladium-catalyzed Negishi cross-coupling reaction involving the commercially available 3-iodo-1H-pyrazole and a benzylzinc bromide derivative, which has been reported to yield up to 82%.[156] However, it is worth noting that the synthesis of the 2,4,5-trimethylphenylzinc bromide coupling partner, though commercially procurable, is protected by patents and thus not readily accessible for research groups. Moving on to the second potential step, it entails the oxidation of p-xylene to terephthalic acid following the Amoco process.[157] It is noteworthy that this oxidation process employs acetic acid as a solvent, compressed oxygen at approximately 200 °C, and a combination of cobalt, manganese, and bromide catalysts. These rigorous synthetic conditions raise concerns regarding the potential undesired oxidation of the benzylic position within the linker precursor, consequently leading to the decomposition of the intended motif.[158] Lastly, the borylation of the pyrazole moiety has been reported utilizing a two-step methodology, which involves the quantitative utilization of an additional BCF:carbene adduct.[150] Furthermore, it is important to acknowledge that this step relies on heterogeneous solid-liquid reactivity occurring at the interface of the MOF. It also requires to simultaneously ensure the stability of the HBF_2 reactant against the reactivity of the Zr-OH groups present on the MOF's surface, as well as any pending carboxylic acid defects. This presents a significant challenge due to the potential risk of hydrolysis [159,160] and the subsequent release of highly toxic hydrofluoric acid and fluoroboric acid, particularly given the potential diffusion limitations within the pores of the MOF.

Anticipating these synthetic limitations by computational approaches is extremely challenging. Consequently, the discovery of heterogenized FLP systems currently relies on the "trial-and-error" explorations of porous matrices from a broad range of potential candidates. However, the knowledge gained from both homogenous systems and theoretically derived structure-activity relationships can be used to narrow the range of FLP candidates to be immobilized, thus saving time consuming experimental efforts. Future work may explore potential synergies between the chemistry of organic linkers and their functionalization, and that of metal nodes in MOFs[72,73] towards the construction of heterogeneous FLPs, which are still rather scarcely covered. Current developments in the field of hybrid porous materials hold the potential to make it possible to achieve unequaled FLP-based heterogeneous catalysts with the only limit being the synthetic capacity to prepare their elementary building blocks.

4.3 Towards catalytic systems

From the computations performed, the first and main assumption made was that the FLP was designed to act as a catalyst, i.e. a species used in an understoichiometric amount to allow a chemical reaction to proceed, often faster, and which remains unchanged at the end of the reaction. However, in most of the systems reported, the final product of the hydrogenation of CO_2 was an adduct with the Lewis acid or base and the organic hydrogenation target (formic acid,

methanol,…) was finally released after hydrolysis. For example, in the work by Zhao[50] and Corminbœuf,[51] the catalytic activity referred to the moles of formate salt of the protonated Lewis base per mole of Lewis acid. The two studies reported the use of a large excess of Lewis base of 10'000 [50] and 100 equivalents [51] compared to the Lewis acid, these systems being however catalytic with respect to the Lewis acid with calculated TONs of 4000 and 24, respectively. As demonstrated by Dyson and Corminbœuf,[51] the release of the formate being the limiting step, the use of excess Lewis base is aimed at displacing the equilibrium towards higher CO_2 conversions. These pioneering studies underscore the potential for innovative catalytic systems by highlighting the importance of optimizing the ratio of Lewis acids and bases to achieve efficient CO_2 hydrogenation. The progress made in understanding and fine-tuning these FLP systems pave the way for future research and development in the field.

4.4 Future developments in computational approaches

There have been a few in-depth DFT studies on solids (periodic calculations or cluster-based simulations) using AIMD and free energy reaction profiles for CO_2 hydrogenation. Limitations issues are related to the size of the crystal structure under study. Most studies use UiO-66 or UiO-67 which could be easily handled using their primitive cells. The same approaches might become much more demanding when turning to MOF possessing larger cell sizes and pores (MIL-101, MIL-100 for instance, PCN-777, MOF-808 etc…). Notably, there is currently a blind spot in computational approaches for considering the dynamical behavior of FLPs once grafted or immobilized into a porous host. Such dynamic approaches are however required in order to predict the positioning of the FLPs within the porous host and to restrict the choice of hosts to those allowing the reactivity of the targeted FLPs to be maintained (minimal pore size, confinement effect,[161] first coordination sphere interactions with the MOF inorganic sub-network through hydrogen bonding or electrostatics, role of defects). So far, there is no reported theoretical study exploring the participation of the MOF itself in the catalysis as a Lewis partner, typically using open metal sites as acid partners, while facing a grafted basic partner, or vice versa.

The mapping of crossed activity is a significant and achievable milestone. The next frontier is the computational exploration of functionalized MOFs, including the partitioning of multiple LA and LB grafts, as well as their dynamics within porous matrices. With the advanced capabilities of numerous force fields and QM/MM techniques, studying the realistic implantation of such LA/LB pairs is well within reach, promising groundbreaking developments in this field.

5. Conclusions

In conclusion, the last years have seen the tremendous development of molecular FLPs for CO_2 hydrogenation, including both experimental and computational advances, with pioneering achievements. Key insights into reaction mechanisms and the factors influencing the reactivity of FLPs towards H_2 splitting and subsequent CO_2 hydrogenation have been obtained from both experimental and computational studies on molecular FLPs. These have laid the groundwork for developing structure-activity relationships, providing guidelines on how to tune the structural and electronic properties of FLPs to achieve efficient CO_2 hydrogenation. Notably, this knowledge can be applied not only to the rational design of molecular FLPs but also to the identification of promising candidates for incorporation into the structure of porous matrices to develop heterogeneous catalysts. However, while the synergy between experimental findings and computations holds the potential to accelerate the discovery of new catalytic FLP systems, examples that leverage the currently available design rules to successfully develop new FLPs for CO_2 hydrogenation are still rare. While computational evaluation provides a trend for optimal geometry and reactivity, experimental expertise is key to determine the feasibility of the FLPs' synthesis and to unravel adequate catalytic conditions.

These challenges become even more complex when transitioning to porous solids through the heterogenization of FLPs. This heterogenization should enable precise control over the FLP's geometry, reactivity, and synergistic effects such as enhancing reactant concentrations locally. Recent pioneering examples already installed a dialogue between computations and experimentations but the implementation of computationally designed in experimentally constructed FLP still require intensive efforts for their in catalytic applications. The development of computational methodologies to go even deeper into the predictions of the synthetic and catalytic conditions combined with the proliferation of synthesis methods based on almost infinite variations of compositions and structures of porous hybrid solids is aimed to push the limits of current systems. Given the evolving nature of this research field, the collaborative efforts of synthetic and computational chemistry are poised to yield sustainable FLP-based catalytic systems for direct CO_2 hydrogenation in the foreseeable future.

Conflicts of interest

There are no conflicts to declare.

Data Availability

No primary research results, software or code have been included and no new data were generated or analysed as part of this review.

Acknowledgements

This work was supported by the French National Agency as part of the program No. ANR-21-CE07-0028. A.S.-D. also acknowledges the Spanish Ministry of Universities and the European Union - Next Generation EU for financial support through a Margarita Salas grant.

References

(1) Hübner, S.; de Vries, J. G.; Farina, V. Why Does Industry Not Use Immobilized Transition Metal Complexes as Catalysts? *Adv. Synth. Catal.* **2016**, *358* (1), 3–25. https://doi.org/10.1002/adsc.201500846.

(2) Artz, J.; Müller, T. E.; Thenert, K.; Kleinekorte, J.; Meys, R.; Sternberg, A.; Bardow, A.; Leitner, W. Sustainable Conversion of Carbon Dioxide: An Integrated Review of Catalysis and Life Cycle Assessment. *Chem. Rev.* **2018**, *118* (2), 434–504. https://doi.org/10.1021/acs.chemrev.7b00435.

(3) Gaich, T.; Baran, P. S. Aiming for the Ideal Synthesis. *J. Org. Chem.* **2010**, *75* (14), 4657–4673. https://doi.org/10.1021/jo1006812.

(4) Welch, G. C.; Juan, R. R. S.; Masuda, J. D.; Stephan, D. W. Reversible, Metal-Free Hydrogen Activation. *Science* **2006**, *314* (5802), 1124–1126. https://doi.org/10.1126/science.1134230.

(5) Navarro, M.; Moreno, J. J.; Campos, J. Frustrated Lewis Pair Systems. In *Comprehensive Organometallic Chemistry IV*; **2022**; Vol. 10, pp 523–616.

(6) Paradies, J. From Structure to Novel Reactivity in Frustrated Lewis Pairs. *Coord. Chem. Rev.* **2019**, *380*, 170–183. https://doi.org/10.1016/j.ccr.2018.09.014.

(7) Frenette, B. L.; Rivard, E. Frustrated Lewis Pair Chelation in the P-Block. *Chem. – Eur. J.* **2023**, *29* (65), e202302332. https://doi.org/10.1002/chem.202302332.

(8) Stephan, D. W.; Erker, G. Frustrated Lewis Pair Chemistry of Carbon, Nitrogen and Sulfur Oxides. *Chem. Sci.* **2014**, *5* (7), 2625–2641. https://doi.org/10.1039/C4SC00395K.

(9) Stephan, D. W. Frustrated Lewis Pairs: From Concept to Catalysis. *Acc. Chem. Res.* **2015**, *48* (2), 306–316. https://doi.org/10.1021/ar500375j.

(10) Khan, M. N.; Ingen, Y. van; Boruah, T.; McLauchlan, A.; Wirth, T.; Melen, R. L. Advances in CO_2 Activation by Frustrated Lewis Pairs: From Stoichiometric to Catalytic Reactions. *Chem. Sci.* **2023**, *14* (47), 13661–13695. https://doi.org/10.1039/D3SC03907B.

(11) Pérez-Jiménez, M.; Corona, H.; de la Cruz-Martínez, F.; Campos, J. Donor-Acceptor Activation of Carbon Dioxide. *Chem. – Eur. J.* **2023**, *29* (61), e202301428. https://doi.org/10.1002/chem.202301428.

(12) Scott, D. J.; Fuchter, M. J.; Ashley, A. E. Designing Effective 'Frustrated Lewis Pair' Hydrogenation Catalysts. *Chem. Soc. Rev.* **2017**, *46* (19), 5689–5700. https://doi.org/10.1039/C7CS00154A.

(13) Fontaine, F.-G.; Courtemanche, M.-A.; Légaré, M.-A.; Rochette, É. Design Principles in Frustrated Lewis Pair Catalysis for the Functionalization of Carbon Dioxide and Heterocycles. *Coord. Chem. Rev.* **2017**, *334*, 124–135. https://doi.org/10.1016/j.ccr.2016.05.005.

(14) Jupp, A. R.; Stephan, D. W. New Directions for Frustrated Lewis Pair Chemistry. *Trends Chem.* **2019**, *1* (1), 35–48. https://doi.org/10.1016/j.trechm.2019.01.006.

(15) Ma, Y.; Zhang, S.; Chang, C.-R.; Huang, Z.-Q.; Ho, J. C.; Qu, Y. Semi-Solid and Solid Frustrated Lewis Pair Catalysts. *Chem. Soc. Rev.* **2018**, *47* (15), 5541–5553. https://doi.org/10.1039/C7CS00691H.

(16) Burai Patrascu, M.; Pottel, J.; Pinus, S.; Bezanson, M.; Norrby, P.-O.; Moitessier, N. From Desktop to Benchtop with Automated Computational Workflows for Computer-Aided Design in Asymmetric Catalysis. *Nat. Catal.* **2020**, *3* (7), 574–584. https://doi.org/10.1038/s41929-020-0468-3.

(17) Rosales, A. R.; Wahlers, J.; Limé, E.; Meadows, R. E.; Leslie, K. W.; Savin, R.; Bell, F.; Hansen, E.; Helquist, P.; Munday, R. H.; Wiest, O.; Norrby, P.-O. Rapid Virtual Screening of Enantioselective Catalysts Using CatVS. *Nat. Catal.* **2019**, *2* (1), 41–45. https://doi.org/10.1038/s41929-018-0193-3.

(18) Rosales, A. R.; Quinn, T. R.; Wahlers, J.; Tomberg, A.; Zhang, X.; Helquist, P.; Wiest, O.; Norrby, P.-O. Application of Q2MM to Predictions in Stereoselective Synthesis. *Chem. Commun.* **2018**, *54* (60), 8294–8311. https://doi.org/10.1039/C8CC03695K.

(19) Mialane, P.; Mellot-Draznieks, C.; Gairola, P.; Duguet, M.; Benseghir, Y.; Oms, O.; Dolbecq, A. Heterogenisation of Polyoxometalates and Other Metal-Based Complexes in Metal–Organic Frameworks: From Synthesis to Characterisation and Applications in Catalysis. *Chem. Soc. Rev.* **2021**, *50* (10), 6152–6220. https://doi.org/10.1039/D0CS00323A.

(20) Chen, B. W. J.; Xu, L.; Mavrikakis, M. Computational Methods in Heterogeneous Catalysis. *Chem. Rev.* **2021**, *121* (2), 1007–1048. https://doi.org/10.1021/acs.chemrev.0c01060.

(21) Shen, X.; Wang, Z.; Gao, X. J.; Gao, X. Reaction Mechanisms and Kinetics of Nanozymes: Insights from Theory and Computation. *Adv. Mater.* **2024**, 36 (10), 2211151. https://doi.org/10.1002/adma.202211151.

(22) Sit, P.; Zhang, L. Density Functional Theory in Heterogeneous Catalysis. In *Heterogeneous Catalysts*; John Wiley & Sons, Ltd, 2021; pp 405–418. https://doi.org/10.1002/9783527813599.ch23.

(23) Stephan, D. W. Catalysis, FLPs, and Beyond. *Chem* **2020**, *6* (7), 1520–1526. https://doi.org/10.1016/j.chempr.2020.05.007.

(24) P., S.; Mandal, S. K. From CO_2 Activation to Catalytic Reduction: A Metal-Free Approach. *Chem. Sci.* **2020**, *11* (39), 10571–10593. https://doi.org/10.1039/D0SC03528A.

(25) Li, N.; Zhang, W. Frustrated Lewis Pairs: Discovery and Overviews in Catalysis. *Chin. J. Chem.* **2020**, *38* (11), 1360–1370. https://doi.org/10.1002/cjoc.202000027.

(26) Lam, J.; Szkop, K. M.; Mosaferi, E.; Stephan, D. W. FLP Catalysis: Main Group Hydrogenations of Organic Unsaturated Substrates. *Chem. Soc. Rev.* **2019**, *48* (13), 3592–3612. https://doi.org/10.1039/C8CS00277K.

(27) Chen, M.; Wang, M.; Ji, M. Design and Synthesis of Heterogeneous Frustrated Lewis Pairs for Hydrogenation: From Molecular Immobilization to Defects Engineering. *ChemCatChem* **2023**, e202301472. https://doi.org/10.1002/cctc.202301472.

(28) Zhang, Y.; Lan, P. C.; Martin, K.; Ma, S. Porous Frustrated Lewis Pair Catalysts: Advances and Perspective. *Chem Catal.* **2022**, *2* (3), 439–457. https://doi.org/10.1016/j.checat.2021.12.001.

(29) Sharma, G.; Newman, P. D.; Platts, J. A. A Review of Quantum Chemical Studies of Frustrated Lewis Pairs. *J. Mol. Graph. Model.* **2021**, *105*, 107846. https://doi.org/10.1016/j.jmgm.2021.107846.

(30) Fontaine, F.-G.; Rochette, É. Ambiphilic Molecules: From Organometallic Curiosity to Metal-Free Catalysts. *Acc. Chem. Res.* **2018**, *51* (2), 454–464. https://doi.org/10.1021/acs.accounts.7b00514.

(31) Ashley, A. E.; Thompson, A. L.; O'Hare, D. Non-Metal-Mediated Homogeneous Hydrogenation of CO_2 to CH_3OH. *Angew. Chem. Int. Ed.* **2009**, *48* (52), 9839–9843. https://doi.org/10.1002/anie.200905466.

(32) Courtemanche, M.-A.; Pulis, A. P.; Rochette, É.; Légaré, M.-A.; Stephan, D. W.; Fontaine, F.-G. Intramolecular B/N Frustrated Lewis Pairs and the Hydrogenation of Carbon Dioxide. *Chem. Commun.* **2015**, *51* (48), 9797–9800. https://doi.org/10.1039/C5CC03072B.

(33) Fontaine, F.-G.; Stephan, D. W. Metal-Free Reduction of CO_2. *Curr. Opin. Green Sustain. Chem.* **2017**, *3*, 28–32. https://doi.org/10.1016/j.cogsc.2016.11.004.

(34) Massey, A. G.; Park, A. J.; Stone, F. G. A. Tris(Pentafluorophenyl)Boron. *Proc. Chem. Soc.* **1963**, 212–213. https://doi.org/10.1002/anie.201704097

(35) Massey, A. G.; Park, A. J. Perfluorophenyl Derivatives of the Elements: I. Tris(Pentafluorophenyl)Boron. *J. Organomet. Chem.* **1964**, *2* (3), 245–250. https://doi.org/10.1016/S0022-328X(00)80518-5.

(36) Piers, W. E.; Chivers, T. Pentafluorophenylboranes: From Obscurity to Applications. *Chem. Soc. Rev.* **1997**, *26* (5), 345–354. https://doi.org/10.1039/CS9972600345.

(37) Erker, G. Tris(Pentafluorophenyl)Borane: A Special Boron Lewis Acid for Special Reactions. *Dalton Trans.* **2005**, *2005*, 1883–1890. https://doi.org/10.1039/B503688G.

(38) Carden, J. L.; Dasgupta, A.; Melen, R. L. Halogenated Triarylboranes: Synthesis, Properties and Applications in Catalysis. *Chem. Soc. Rev.* **2020**, *49* (6), 1706–1725. https://doi.org/10.1039/C9CS00769E.

(39) Mömming, C. M.; Otten, E.; Kehr, G.; Fröhlich, R.; Grimme, S.; Stephan, D. W.; Erker, G. Reversible Metal-Free Carbon Dioxide Binding by Frustrated Lewis Pairs. *Angew. Chem. Int. Ed.* **2009**, *48* (36), 6643–6646. https://doi.org/10.1002/anie.200901636.

(40) Sumerin, V.; Schulz, F.; Nieger, M.; Leskelä, M.; Repo, T.; Rieger, B. Facile Heterolytic H_2 Activation by Amines and $B(C_6F_5)_3$. *Angew. Chem. Int. Ed.* **2008**, *47* (32), 6001–6003. https://doi.org/10.1002/anie.200800935.

(41) Liu, L.; Vankova, N.; Heine, T. A Kinetic Study on the Reduction of CO_2 by Frustrated Lewis Pairs: From Understanding to Rational Design. *Phys. Chem. Chem. Phys.* **2016**, *18* (5), 3567–3574. https://doi.org/10.1039/C5CP06925D.

(42) Wang, H.; Zhao, Y.; Zhao, H.; Yang, J.; Zhai, D.; Sun, L.; Deng, W. In Silico Design of Metal-Free Hydrophosphate Catalysts for Hydrogenation of CO_2 to Formate. *Phys. Chem. Chem. Phys.* **2022**, *24* (5), 2901–2908. https://doi.org/10.1039/D1CP04582B.

(43) Tran, S. D.; Tronic, T. A.; Kaminsky, W.; Michael Heinekey, D.; Mayer, J. M. Metal-Free Carbon Dioxide Reduction and Acidic C–H Activations Using a Frustrated Lewis Pair. *Inorganica Chim. Acta* **2011**, *369* (1), 126–132. https://doi.org/10.1016/j.ica.2010.12.022.

(44) Voss, T.; Mahdi, T.; Otten, E.; Fröhlich, R.; Kehr, G.; Stephan, D. W.; Erker, G. Frustrated Lewis Pair Behavior of Intermolecular Amine/$B(C_6F_5)_3$ Pairs. *Organometallics* **2012**, *31* (6), 2367–2378. https://doi.org/10.1021/om300017u.

(45) Travis, A. L.; Binding, S. C.; Zaher, H.; Arnold, T. A. Q.; Buffet, J.-C.; O'Hare, D. Small Molecule Activation by Frustrated Lewis Pairs. *Dalton Trans.* **2013**, *42* (7), 2431–2437. https://doi.org/10.1039/C2DT32525J.

(46) Ménard, G.; Stephan, D. W. Room Temperature Reduction of CO_2 to Methanol by Al-Based Frustrated Lewis Pairs and Ammonia Borane. *J. Am. Chem. Soc.* **2010**, *132* (6), 1796–1797. https://doi.org/10.1021/ja9104792.

(47) Ménard, G.; Stephan, D. W. Stoichiometric Reduction of CO_2 to CO by Aluminum-Based Frustrated Lewis Pairs. *Angew. Chem. Int. Ed.* **2011**, *50* (36), 8396–8399. https://doi.org/10.1002/anie.201103600.

(48) Zall, C. M.; Linehan, J. C.; Appel, A. M. A Molecular Copper Catalyst for Hydrogenation of CO_2 to Formate. *ACS Catal.* **2015**, *5* (9), 5301–5305. https://doi.org/10.1021/acscatal.5b01646.

(49) Wickemeyer, L.; Aders, N.; Mix, A.; Neumann, B.; Stammler, H.-G.; Cabrera-Trujillo, J. J.; Fernández, I.; Mitzel, N. W. Carbon Dioxide Reduction by an Al–O–P Frustrated Lewis Pair. *Chem. Sci.* **2022**, *13* (27), 8088–8094. https://doi.org/10.1039/D2SC01870E.

(50) Zhao, T.; Hu, X.; Wu, Y.; Zhang, Z. Hydrogenation of CO_2 to Formate with H_2: Transition Metal Free Catalyst Based on a Lewis Pair. *Angew. Chem. Int. Ed.* **2019**, *58* (3), 722–726. https://doi.org/10.1002/anie.201809634.

(51) Das, S.; Turnell-Ritson, R. C.; Dyson, P. J.; Corminboeuf, C. Design of Frustrated Lewis Pair Catalysts for Direct Hydrogenation of CO_2. *Angew. Chem. Int. Ed.* **2022**, *61* (46), e202208987. https://doi.org/10.1002/anie.202208987.

(52) Geier, S. J.; Stephan, D. W. Lutidine/$B(C_6F_5)_3$: At the Boundary of Classical and Frustrated Lewis Pair Reactivity. *J. Am. Chem. Soc.* **2009**, *131* (10), 3476–3477. https://doi.org/10.1021/ja900572x.

(53) Rokob, T. A.; Hamza, A.; Pápai, I. Rationalizing the Reactivity of Frustrated Lewis Pairs: Thermodynamics of H_2 Activation and the Role of Acid−Base Properties. *J. Am. Chem. Soc.* **2009**, *131* (30), 10701–10710. https://doi.org/10.1021/ja903878z.

(54) Peuser, I.; Neu, R. C.; Zhao, X.; Ulrich, M.; Schirmer, B.; Tannert, J. A.; Kehr, G.; Fröhlich, R.; Grimme, S.; Erker, G.; Stephan, D. W. CO_2 and Formate Complexes of Phosphine/Borane Frustrated Lewis Pairs. *Chem. – Eur. J.* **2011**, *17* (35), 9640–9650. https://doi.org/10.1002/chem.201100286.

(55) Welch, G. C.; Stephan, D. W. Facile Heterolytic Cleavage of Dihydrogen by Phosphines and Boranes. *J. Am. Chem. Soc.* **2007**, *129* (7), 1880–1881. https://doi.org/10.1021/ja067961j.

(56) Binding, S. C.; Zaher, H.; Chadwick, F. M.; O'Hare, D. Heterolytic Activation of Hydrogen Using Frustrated Lewis Pairs Containing Tris(2,2′,2″-Perfluorobiphenyl)Borane. *Dalton Trans.* **2012**, *41* (30), 9061–9066. https://doi.org/10.1039/C2DT30334E.

(57) Zhao, X.; Stephan, D. W. Bis-Boranes in the Frustrated Lewis Pair Activation of Carbon Dioxide. *Chem. Commun.* **2011**, *47* (6), 1833–1835. https://doi.org/10.1039/C0CC04791K.

(58) Sgro, M. J.; Dömer, J.; Stephan, D. W. Stoichiometric CO_2 Reductions Using a Bis-Borane-Based Frustrated Lewis Pair. *Chem. Commun.* **2012**, *48* (58), 7253–7255. https://doi.org/10.1039/C2CC33301E.

(59) Weicker, S. A.; Stephan, D. W. Activation of Carbon Dioxide by Silyl Triflate-Based Frustrated Lewis Pairs. *Chem. – Eur. J.* **2015**, *21* (37), 13027–13034. https://doi.org/10.1002/chem.201501904.

(60) Stephan, D. W. Frustrated Lewis Pairs. *J. Am. Chem. Soc.* **2015**, *137* (32), 10018–10032. https://doi.org/10.1021/jacs.5b06794.

(61) Jiang, Y.; Blacque, O.; Fox, T.; Berke, H. Catalytic CO_2 Activation Assisted by Rhenium Hydride/$B(C_6F_5)_3$ Frustrated Lewis Pairs—Metal Hydrides Functioning as FLP Bases. *J. Am. Chem. Soc.* **2013**, *135* (20), 7751–7760. https://doi.org/10.1021/ja402381d.

(62) Courtemanche, M.-A.; Légaré, M.-A.; Maron, L.; Fontaine, F.-G. A Highly Active Phosphine–Borane Organocatalyst for the Reduction of CO_2 to Methanol Using Hydroboranes. *J. Am. Chem. Soc.* **2013**, *135* (25), 9326–9329. https://doi.org/10.1021/ja404585p.

(63) Courtemanche, M.-A.; Légaré, M.-A.; Maron, L.; Fontaine, F.-G. Reducing CO_2 to Methanol Using Frustrated Lewis Pairs: On the Mechanism of Phosphine–Borane-Mediated Hydroboration of CO_2. *J. Am. Chem. Soc.* **2014**, *136* (30), 10708–10717. https://doi.org/10.1021/ja5047846.

(64) Courtemanche, M.-A.; Larouche, J.; Légaré, M.-A.; Bi, W.; Maron, L.; Fontaine, F.-G. A Tris(Triphenylphosphine)Aluminum Ambiphilic Precatalyst for the Reduction of Carbon Dioxide with Catecholborane. *Organometallics* **2013**, *32* (22), 6804–6811. https://doi.org/10.1021/om400645s.

(65) Declercq, R.; Bouhadir, G.; Bourissou, D.; Légaré, M.-A.; Courtemanche, M.-A.; Nahi, K. S.; Bouchard, N.; Fontaine, F.-G.; Maron, L. Hydroboration of Carbon Dioxide Using Ambiphilic Phosphine–Borane Catalysts: On the Role of the Formaldehyde Adduct. *ACS Catal.* **2015**, *5* (4), 2513–2520. https://doi.org/10.1021/acscatal.5b00189.

(66) Krämer, F.; Paradies, J.; Fernández, I.; Breher, F. Quo Vadis CO_2 Activation: Catalytic Reduction of CO_2 to Methanol Using Aluminum and Gallium/Carbon-Based Ambiphiles. *Chem. – Eur. J.* **2024**, *30* (5), e202303380. https://doi.org/10.1002/chem.202303380.

(67) Wang, T.; Stephan, D. W. Phosphine Catalyzed Reduction of CO_2 with Boranes. *Chem. Commun.* **2014**, *50* (53), 7007–7010. https://doi.org/10.1039/C4CC02103G.

(68) Das, S.; Laplaza, R.; Blaskovits, J. T.; Corminboeuf, C. Mapping Active Site Geometry to Activity in Immobilized Frustrated Lewis Pair Catalysts. *Angew. Chem. Int. Ed.* **2022**, *61* (32). https://doi.org/10.1002/anie.202202727.

(69) Szeto, K. C.; Sahyoun, W.; Merle, N.; Castelbou, J. L.; Popoff, N.; Lefebvre, F.; Raynaud, J.; Godard, C.; Claver, C.; Delevoye, L.; Gauvin, R. M.; Taoufik, M. Development of Silica-Supported Frustrated Lewis Pairs: Highly Active Transition Metal-Free Catalysts for the Z-Selective Reduction of Alkynes. *Catal. Sci. Technol.* **2016**, *6* (3), 882–889. https://doi.org/10.1039/C5CY01372K.

(70) Xing, J.-Y.; Buffet, J.-C.; Rees, N. H.; Nørby, P.; O'Hare, D. Hydrogen Cleavage by Solid-Phase Frustrated Lewis Pairs. *Chem. Commun.* **2016**, *52* (69), 10478–10481. https://doi.org/10.1039/C6CC04937K.

(71) Mentoor, K.; Twigge, L.; Niemantsverdriet, J. W. H.; Swarts, J. C.; Erasmus, E. Silica Nanopowder Supported Frustrated Lewis Pairs for CO_2 Capture and Conversion to Formic Acid. *Inorg. Chem.* **2021**, *60* (1), 55–69. https://doi.org/10.1021/acs.inorgchem.0c02012.

(72) Niu, Z.; Zhang, W.; Lan, P. C.; Aguila, B.; Ma, S. Promoting Frustrated Lewis Pairs for Heterogeneous Chemoselective Hydrogenation via the Tailored Pore Environment within Metal–Organic Frameworks. *Angew. Chem. Int. Ed.* **2019**, *58* (22), 7420–7424. https://doi.org/10.1002/anie.201903763.

(73) Niu, Z.; Bhagya Gunatilleke, W. D. C.; Sun, Q.; Lan, P. C.; Perman, J.; Ma, J.-G.; Cheng, Y.; Aguila, B.; Ma, S. Metal-Organic Framework Anchored with a Lewis Pair as a New Paradigm for Catalysis. *Chem* **2018**, *4* (11), 2587–2599. https://doi.org/10.1016/j.chempr.2018.08.018.

(74) Shyshkanov, S.; Nguyen, T. N.; Ebrahim, F. M.; Stylianou, K. C.; Dyson, P. J. In Situ Formation of Frustrated Lewis Pairs in a Water-Tolerant Metal-Organic Framework for the Transformation of CO_2. *Angew. Chem. Int. Ed.* **2019**, *58* (16), 5371–5375. https://doi.org/10.1002/anie.201901171.

(75) Shyshkanov, S.; Nguyen, T. N.; Chidambaram, A.; Stylianou, K. C.; Dyson, P. J. Frustrated Lewis Pair-Mediated Fixation of CO_2 within a Metal–Organic Framework. *Chem. Commun.* **2019**, *55* (73), 10964–10967. https://doi.org/10.1039/C9CC04374H.

(76) Zhang, Y.; Chen, S.; Al-Enizi, A. M.; Nafady, A.; Tang, Z.; Ma, S. Chiral Frustrated Lewis Pair@Metal-Organic Framework as a New Platform for Heterogeneous Asymmetric Hydrogenation. *Angew. Chem. Int. Ed.* **2023**, *62* (2), e202213399. https://doi.org/10.1002/anie.202213399.

(77) Trunk, M.; Teichert, J. F.; Thomas, A. Room-Temperature Activation of Hydrogen by Semi-Immobilized Frustrated Lewis Pairs in Microporous Polymer Networks. *J. Am. Chem. Soc.* **2017**, *139* (10), 3615–3618. https://doi.org/10.1021/jacs.6b13147.

(78) Willms, A.; Schumacher, H.; Tabassum, T.; Qi, L.; Scott, S. L.; Hausoul, P. J. C.; Rose, M. Solid Molecular Frustrated Lewis Pairs in a Polyamine Organic Framework for the Catalytic Metal-Free Hydrogenation of Alkenes. *ChemCatChem* **2018**, *10* (8), 1835–1843. https://doi.org/10.1002/cctc.201701783.

(79) Chen, L.; Liu, R.; Yan, Q. Polymer Meets Frustrated Lewis Pair: Second-Generation CO_2-Responsive Nanosystem for Sustainable CO_2 Conversion. *Angew. Chem. Int. Ed.* **2018**, *57* (30), 9336–9340. https://doi.org/10.1002/anie.201804034.

(80) Hou, L.; Liang, Y.; Wang, Q.; Zhang, Y.; Dong, D.; Zhang, N. Lewis Pair-Mediated Surface-Initiated Polymerization. *ACS Macro Lett.* **2018**, *7* (1), 65–69. https://doi.org/10.1021/acsmacrolett.7b00903.

(81) Maina, J. W.; Pozo-Gonzalo, C.; Kong, L.; Schütz, J.; Hill, M.; Dumée, L. F. Metal Organic Framework Based Catalysts for CO_2 Conversion. *Mater. Horiz.* **2017**, *4* (3), 345–361. https://doi.org/10.1039/C6MH00484A.

(82) Canivet, J.; Wisser, F. M. Metal–Organic Framework Catalysts for Solar Fuels: Light-Driven Conversion of Carbon Dioxide into Formic Acid. *ACS Appl. Energy Mater.* **2023**, *6* (18), 9027–9043 https://doi.org/10.1021/acsaem.2c03731.

(83) Beyzavi, H.; Klet, R. C.; Tussupbayev, S.; Borycz, J.; Vermeulen, N. A.; Cramer, C. J.; Stoddart, J. F.; Hupp, J. T.; Farha, O. K. A Hafnium-Based Metal–Organic Framework as an Efficient and Multifunctional Catalyst for Facile CO_2 Fixation and Regioselective and Enantioretentive Epoxide Activation. *J. Am. Chem. Soc.* **2014**, *136* (45), 15861–15864. https://doi.org/10.1021/ja508626n.

(84) Gao, W.-Y.; Chen, Y.; Niu, Y.; Williams, K.; Cash, L.; Perez, P. J.; Wojtas, L.; Cai, J.; Chen, Y.-S.; Ma, S. Crystal Engineering of an Nbo Topology Metal–Organic Framework for Chemical Fixation of CO_2 under Ambient Conditions. *Angew. Chem. Int. Ed.* **2014**, *53* (10), 2615–2619. https://doi.org/10.1002/anie.201309778.

(85) Sumida, K.; Rogow, D. L.; Mason, J. A.; McDonald, T. M.; Bloch, E. D.; Herm, Z. R.; Bae, T.-H.; Long, J. R. Carbon Dioxide Capture in Metal–Organic Frameworks. *Chem. Rev.* **2012**, *112* (2), 724–781. https://doi.org/10.1021/cr2003272.

(86) Ji, Z.; Wang, H.; Canossa, S.; Wuttke, S.; Yaghi, O. M. Pore Chemistry of Metal–Organic Frameworks. *Adv. Funct. Mater.* **2020**, *30* (41), 2000238. https://doi.org/10.1002/adfm.202000238.

(87) Dutta, A.; Pan, Y.; Liu, J.-Q.; Kumar, A. Multicomponent Isoreticular Metal-Organic Frameworks: Principles, Current Status and Challenges. *Coord. Chem. Rev.* **2021**, *445*, 214074. https://doi.org/10.1016/j.ccr.2021.214074.

(88) Ye, J.; Johnson, J. K. Design of Lewis Pair-Functionalized Metal Organic Frameworks for CO_2 Hydrogenation. *ACS Catal.* **2015**, *5* (5), 2921–2928. https://doi.org/10.1021/acscatal.5b00396.

(89) Ye, J.; Johnson, J. K. Screening Lewis Pair Moieties for Catalytic Hydrogenation of CO_2 in Functionalized UiO-66. *ACS Catal.* **2015**, *5* (10), 6219–6229. https://doi.org/10.1021/acscatal.5b01191.

(90) Ye, J.; Johnson, J. K. Catalytic Hydrogenation of CO_2 to Methanol in a Lewis Pair Functionalized MOF. *Catal. Sci. Technol.* **2016**, *6* (24), 8392–8405. https://doi.org/10.1039/C6CY01245K.

(91) Ye, J.; Yeh, B. Y.; Reynolds, R. A.; Johnson, J. K. Screening the Activity of Lewis Pairs for Hydrogenation of CO_2. *Mol. Simul.* **2017**, *43* (10–11), 821–827. https://doi.org/10.1080/08927022.2017.1295457.

(92) Ye, J.; Li, L.; Johnson, J. K. The Effect of Topology in Lewis Pair Functionalized Metal Organic Frameworks on CO_2 Adsorption and Hydrogenation. *Catal. Sci. Technol.* **2018**, *8* (18), 4609–4617. https://doi.org/10.1039/C8CY01018H.

(93) Heshmat, M. Alternative Pathway of CO_2 Hydrogenation by Lewis-Pair-Functionalized UiO-66 MOF Revealed by Metadynamics Simulations. *J. Phys. Chem. C* **2020**, *124* (20), 10951–10960. https://doi.org/10.1021/acs.jpcc.0c01088.

(94) Férey, G.; Mellot-Draznieks, C.; Serre, C.; Millange, F.; Dutour, J.; Surblé, S.; Margiolaki, I. A Chromium Terephthalate-Based Solid with Unusually Large Pore Volumes and Surface Area. *Science* **2005**, *309* (5743), 2040–2042. https://doi.org/10.1126/science.1116275.

(95) Liu, Q.; Liao, Q.; Hu, J.; Xi, K.; Wu, Y.; Hu, X. Covalent Organic Frameworks Anchored with Frustrated Lewis Pairs for Hydrogenation of Alkynes with H_2. *J. Mater. Chem. A* **2022**, *10* (13), 7333–7340. https://doi.org/10.1039/D1TA08916A.

(96) Zakharova, M. V.; Masoumifard, N.; Hu, Y.; Han, J.; Kleitz, F.; Fontaine, F.-G. Designed Synthesis of Mesoporous Solid-Supported Lewis Acid–Base Pairs and Their CO_2 Adsorption Behaviors. *ACS Appl. Mater. Interfaces* **2018**, *10* (15), 13199–13210. https://doi.org/10.1021/acsami.8b00640.

(97) Yepes, D.; Jaque, P.; Fernández, I. Deeper Insight into the Factors Controlling H_2 Activation by Geminal Aminoborane-Based Frustrated Lewis Pairs. *Chem. - Eur. J.* **2016**, *22* (52), 18801–18809. https://doi.org/10.1002/chem.201603889.

(98) Liu Zeonjuk, L.; St. Petkov, P.; Heine, T.; Röschenthaler, G.-V.; Eicher, J.; Vankova, N. Are Intramolecular Frustrated Lewis Pairs Also Intramolecular Catalysts? A Theoretical Study on H_2 Activation. *Phys. Chem. Chem. Phys.* **2015**, *17* (16), 10687–10698. https://doi.org/10.1039/C5CP00368G.

(99) Rokob, T. A.; Hamza, A.; Stirling, A.; Soós, T.; Pápai, I. Turning Frustration into Bond Activation: A Theoretical Mechanistic Study on Heterolytic Hydrogen Splitting by Frustrated Lewis Pairs. *Angew. Chem. Int. Ed.* **2008**, *47* (13), 2435–2438. https://doi.org/10.1002/anie.200705586.

(100) Guo, Y.; Li, S. Unusual Concerted Lewis Acid−Lewis Base Mechanism for Hydrogen Activation by a Phosphine−Borane Compound. *Inorg. Chem.* **2008**, *47* (14), 6212–6219. https://doi.org/10.1021/ic702489s.

(101) Spies, P.; Erker, G.; Kehr, G.; Bergander, K.; Fröhlich, R.; Grimme, S.; Stephan, D. W. Rapid Intramolecular Heterolytic Dihydrogen Activation by a Four-Membered Heterocyclic Phosphane–Borane Adduct. *Chem. Commun.* **2007**, No. 47, 5072. https://doi.org/10.1039/b710475h.

(102) Spies, P.; Schwendemann, S.; Lange, S.; Kehr, G.; Fröhlich, R.; Erker, G. Metal-Free Catalytic Hydrogenation of Enamines, Imines, and Conjugated Phosphinoalkenylboranes. *Angew. Chem. Int. Ed.* **2008**, *47* (39), 7543–7546. https://doi.org/10.1002/anie.200801432.

(103) Spies, P.; Kehr, G.; Bergander, K.; Wibbeling, B.; Fröhlich, R.; Erker, G. Metal-Free Dihydrogen Activation Chemistry: Structural and Dynamic Features of Intramolecular P/B Pairs. *Dalton Trans.* **2009**, 1534-1541. https://doi.org/10.1039/b815832k.

(104) Grimme, S.; Kruse, H.; Goerigk, L.; Erker, G. The Mechanism of Dihydrogen Activation by Frustrated Lewis Pairs Revisited. *Angew. Chem. Int. Ed.* **2010**, *49* (8), 1402–1405. https://doi.org/10.1002/anie.200905484.

(105) Rokob, T. A.; Bakó, I.; Stirling, A.; Hamza, A.; Pápai, I. Reactivity Models of Hydrogen Activation by Frustrated Lewis Pairs: Synergistic Electron Transfers or Polarization by Electric Field? *J. Am. Chem. Soc.* **2013**, *135* (11), 4425–4437. https://doi.org/10.1021/ja312387q.

(106) Cabrera-Trujillo, J. J.; Fernández, I. Aromaticity Can Enhance the Reactivity of P-Donor/Borole Frustrated Lewis Pairs. *Chem. Commun.* **2019**, *55* (5), 675–678. https://doi.org/10.1039/C8CC09777A.

(107) Pu, M.; Privalov, T. *Ab Initio* Dynamics Trajectory Study of the Heterolytic Cleavage of H2 by a Lewis Acid $[B(C_6F_5)_3]$ and a Lewis Base $[P(t\text{Bu})_3]$. *J. Chem. Phys.* **2013**, *138* (15), 154305. https://doi.org/10.1063/1.4799932.

(108) Pu, M.; Privalov, T. How Frustrated Lewis Acid/Base Systems Pass through Transition-State Regions: H_2 Cleavage by $[t\text{Bu}_3\text{P}/\text{B}(C_6F_5)_3]$. *ChemPhysChem* **2014**, *15* (14), 2936–2944. https://doi.org/10.1002/cphc.201402450.

(109) Pu, M.; Privalov, T. Ab Initio Molecular Dynamics Study of Hydrogen Cleavage by a Lewis Base $[t\text{Bu}_3\ \text{P}]$ and a Lewis Acid $[B(C_6F_5)_3]$ at the Mesoscopic Level-Dynamics in the Solute-Solvent Molecular Clusters. *ChemPhysChem* **2014**, *15* (17), 3714–3719. https://doi.org/10.1002/cphc.201402519.

(110) Pu, M.; Privalov, T. Chemistry of Intermolecular Frustrated Lewis Pairs in Motion: Emerging Perspectives and Prospects. *Isr. J. Chem.* **2015**, *55* (2), 179–195. https://doi.org/10.1002/ijch.201400159.

(111) Liu, L.; Lukose, B.; Ensing, B. Hydrogen Activation by Frustrated Lewis Pairs Revisited by Metadynamics Simulations. *J. Phys. Chem. C* **2017**, *121* (4), 2046–2051. https://doi.org/10.1021/acs.jpcc.6b09991.

(112) Heshmat, M.; Privalov, T. Testing the Nature of Reaction Coordinate Describing Interaction of H_2 with Carbonyl Carbon, Activated by Lewis Acid Complexation, and the Lewis Basic Solvent: A Born-Oppenheimer Molecular Dynamics Study with Explicit Solvent. *J. Chem. Phys.* **2017**, *147* (9), 094302. https://doi.org/10.1063/1.4999708.

(113) Skara, G.; De Vleeschouwer, F.; Geerlings, P.; De Proft, F.; Pinter, B. Heterolytic Splitting of Molecular Hydrogen by Frustrated and Classical Lewis Pairs: A Unified Reactivity Concept. *Sci. Rep.* **2017**, *7* (1), 16024. https://doi.org/10.1038/s41598-017-16244-1.

(114) Heshmat, M.; Ensing, B. Optimizing the Energetics of FLP-Type H_2 Activation by Modulating the Electronic and Structural Properties of the Lewis Acids: A DFT Study. *J. Phys. Chem. A* **2020**, *124* (32), 6399–6410. https://doi.org/10.1021/acs.jpca.0c03108.

(115) Daru, J.; Bakó, I.; Stirling, A.; Pápai, I. Mechanism of Heterolytic Hydrogen Splitting by Frustrated Lewis Pairs: Comparison of Static and Dynamic Models. *ACS Catal.* **2019**, *9* (7), 6049–6057. https://doi.org/10.1021/acscatal.9b01137.

(116) Hamza, A.; Stirling, A.; András Rokob, T.; Pápai, I. Mechanism of Hydrogen Activation by Frustrated Lewis Pairs: A Molecular

Orbital Approach. *Int. J. Quantum Chem.* **2009**, *109* (11), 2416–2425. https://doi.org/10.1002/qua.22203.

(117) Ullrich, M.; Lough, A. J.; Stephan, D. W. Reversible, Metal-Free, Heterolytic Activation of H_2 at Room Temperature. *J. Am. Chem. Soc.* **2009**, *131* (1), 52–53. https://doi.org/10.1021/ja808506t.

(118) Liu, L.; Lukose, B.; Jaque, P.; Ensing, B. Reaction Mechanism of Hydrogen Activation by Frustrated Lewis Pairs. *Green Energy Environ.* **2019**, *4* (1), 20–28. https://doi.org/10.1016/j.gee.2018.06.001.

(119) Stephan, D. W.; Erker, G. Frustrated Lewis Pairs: Metal-Free Hydrogen Activation and More. *Angew. Chem. Int. Ed.* **2010**, *49* (1), 46–76. https://doi.org/10.1002/anie.200903708.

(120) Pérez, P.; Yepes, D.; Jaque, P.; Chamorro, E.; Domingo, L. R.; Rojas, R. S.; Toro-Labbé, A. A Computational and Conceptual DFT Study on the Mechanism of Hydrogen Activation by Novel Frustrated Lewis Pairs. *Phys. Chem. Chem. Phys.* **2015**, *17* (16), 10715–10725. https://doi.org/10.1039/C5CP00306G.

(121) Zhuang, D.; Li, Y.; Zhu, J. Antiaromaticity-Promoted Activation of Dihydrogen with Borole Fused Cyclooctatetraene Frustrated Lewis Pairs: A Density Functional Theory Study. *Organometallics* **2020**, *39* (14), 2636–2641. https://doi.org/10.1021/acs.organomet.0c00263.

(122) Camaioni, D. M.; Ginovska-Pangovska, B.; Schenter, G. K.; Kathmann, S. M.; Autrey, T. Analysis of the Activation and Heterolytic Dissociation of H_2 by Frustrated Lewis Pairs: NH_3/BX_3 (X = H, F, and Cl). *J. Phys. Chem. A* **2012**, *116* (26), 7228–7237. https://doi.org/10.1021/jp3039829.

(123) Zhang, J.; Shao, Y.; Li, Y.; Liu, Y.; Ke, Z. Rational Design of FLP Catalysts for Reversible H_2 Activation: A DFT Study of the Geometric and Electronic Effects. *Chin. Chem. Lett.* **2018**, *29* (8), 1226–1232. https://doi.org/10.1016/j.cclet.2018.02.007.

(124) Kolychev, E. L.; Theuergarten, E.; Tamm, M. N-Heterocyclic Carbenes in FLP Chemistry. In *Frustrated Lewis Pairs II*; Erker, G., Stephan, D. W., Eds.; Topics in Current Chemistry; Springer Berlin Heidelberg: Berlin, Heidelberg, 2012; Vol. 334, pp 121–155. https://doi.org/10.1007/128_2012_379.

(125) Wass, D. F.; Chapman, A. M. Frustrated Lewis Pairs Beyond the Main Group: Transition Metal-Containing Systems. In *Frustrated Lewis Pairs II*; Erker, G., Stephan, D. W., Eds.; Topics in Current Chemistry; Springer Berlin Heidelberg: Berlin, Heidelberg, 2013; Vol. 334, pp 261–280. https://doi.org/10.1007/128_2012_395.

(126) Wan, Q.; Lin, S.; Guo, H. Frustrated Lewis Pairs in Heterogeneous Catalysis: Theoretical Insights. *Molecules* **2022**, *27* (12), 3734. https://doi.org/10.3390/molecules27123734.

(127) Ghuman, K. K.; Hoch, L. B.; Wood, T. E.; Mims, C.; Singh, C. V.; Ozin, G. A. Surface Analogues of Molecular Frustrated Lewis Pairs in Heterogeneous CO_2 Hydrogenation Catalysis. *ACS Catal.* **2016**, *6* (9), 5764–5770. https://doi.org/10.1021/acscatal.6b01015.

(128) Ghoussoub, M.; Yadav, S.; Ghuman, K. K.; Ozin, G. A.; Singh, C. V. Metadynamics-Biased Ab Initio Molecular Dynamics Study of Heterogeneous CO_2 Reduction via Surface Frustrated Lewis Pairs. *ACS Catal.* **2016**, *6* (10), 7109–7117. https://doi.org/10.1021/acscatal.6b01545.

(129) Zeonjuk, L. L.; Vankova, N.; Mavrandonakis, A.; Heine, T.; Röschenthaler, G.; Eicher, J. On the Mechanism of Hydrogen Activation by Frustrated Lewis Pairs. *Chem. – Eur. J.* **2013**, *19* (51), 17413–17424. https://doi.org/10.1002/chem.201302727.

(130) Evans, M. G.; Polanyi, M. Inertia and driving force of chemical reactions. *Soc., Trans. Faraday* **1938**, *34*, 11–24. https://doi.org/10.1039/TF9383400011.

(131) Bronsted, J. N. Acid and Basic Catalysis. *Chem. Rev.* **1928**, *5*, 231–338. https://doi.org/10.1021/cr60019a001.

(132) Jiang, C.; Blacque, O.; Fox, T.; Berke, H. Reversible, Metal-Free Hydrogen activation by Frustrated Lewis Pairs. *Dalton Trans* **2011**, *40* (5), 1091–1097. https://doi.org/10.1039/C0DT01255F.

(133) Dobrovetsky, R.; Stephan, D. W. Catalytic Reduction of CO_2 to CO by Using Zinc(II) and In Situ Generated Carbodiphosphoranes. *Angew. Chem. Int. Ed.* **2013**, *52* (9), 2516–2519. https://doi.org/10.1002/anie.201208817.

(134) Wen, M.; Huang, F.; Lu, G.; Wang, Z.-X. Density Functional Theory Mechanistic Study of the Reduction of CO_2 to CH_4 Catalyzed by an Ammonium Hydridoborate Ion Pair: CO_2 Activation via Formation of a Formic Acid Entity. *Inorg. Chem.* **2013**, *52* (20), 12098–12107. https://doi.org/10.1021/ic401920b.

(135) Zimmerman, P. M.; Zhang, Z.; Musgrave, C. B. Simultaneous Two-Hydrogen Transfer as a Mechanism for Efficient CO_2 Reduction. *Inorg. Chem.* **2010**, *49* (19), 8724–8728. https://doi.org/10.1021/ic100454z.

(136) Jiang, B.; Zhang, Q.; Dang, L. Theoretical Studies on Bridged Frustrated Lewis Pair (FLP) Mediated H_2 Activation and CO_2 Hydrogenation. *Org. Chem. Front.* **2018**, *5* (12), 1905–1915. https://doi.org/10.1039/C8QO00192H.

(137) Delarmelina, M.; Carneiro, J. W. D. M.; Catlow, C. R. A.; Bühl, M. Design of CO_2 Hydrogenation Catalysts Based on Phosphane/Borane Frustrated Lewis Pairs and Xanthene-Derived Scaffolds. *Catal. Commun.* **2022**, *162*, 106385. https://doi.org/10.1016/j.catcom.2021.106385.

(138) Ghara, M.; Pan, S.; Chattaraj, P. K. A Theoretical Investigation on Boron–Ligand Cooperation to Activate Molecular Hydrogen by a Frustrated Lewis Pair and Subsequent Reduction of Carbon Dioxide. *Phys. Chem. Chem. Phys.* **2019**, *21* (38), 21267–21277. https://doi.org/10.1039/C9CP03756J.

(139) Sabet-Sarvestani, H.; Izadyar, M.; Eshghi, H. Molecular Electrostatic Potential at Nuclear Position as a New Concept in Evaluation of the Substitution Effects of Intramolecular B/N Frustrated Lewis Pairs in H_2 Splitting and CO_2 Reduction. *Int. J. Quantum Chem.* **2020**, *120* (24). https://doi.org/10.1002/qua.26416.

(140) Ghara, M.; Chattaraj, P. K. A Computational Study on Hydrogenation of CO_2 Catalyzed by a Bridged B/N Frustrated Lewis Pair. *Struct. Chem.* **2019**, *30* (3), 1067–1077. https://doi.org/10.1007/s11224-018-1264-4.

(141) Mo, Z.; Kolychev, E. L.; Rit, A.; Campos, J.; Niu, H.; Aldridge, S. Facile Reversibility by Design: Tuning Small Molecule Capture and Activation by Single Component Frustrated Lewis Pairs. *J. Am. Chem. Soc.* **2015**, *137* (38), 12227–12230. https://doi.org/10.1021/jacs.5b08614.

(142) Liu, L.; Lukose, B.; Ensing, B. A Free Energy Landscape of CO_2 Capture by Frustrated Lewis Pairs. *ACS Catal.* **2018**, *8* (4), 3376–3381. https://doi.org/10.1021/acscatal.7b04072.

(143) Pu, M.; Privalov, T. Ab Initio Molecular Dynamics with Explicit Solvent Reveals a Two-Step Pathway in the Frustrated Lewis Pair Reaction. *Chem. – Eur. J.* **2015**, *21* (49), 17708–17720. https://doi.org/10.1002/chem.201502926.

(144) Zhang, Z.-F.; Su, M.-D. Theoretical Study of the Activation Reaction of a Zr^+/P-Based Frustrated Lewis Pair with Carbon

Dioxide. *J. Phys. Chem. A* **2022**, *126* (33), 5534–5544. https://doi.org/10.1021/acs.jpca.2c03602.

(145) Ghara, M.; Chattaraj, P. K. Can a Decrease in Anti-Aromaticity Increase the Dihydrogen Activation Ability of a Frustrated Phosphorous/Borane Lewis Pair?: A DFT Study. *Theor. Chem. Acc.* **2020**, *139* (12), 183. https://doi.org/10.1007/s00214-020-02698-6.

(146) Cavka, J. H.; Jakobsen, S.; Olsbye, U.; Guillou, N.; Lamberti, C.; Bordiga, S.; Lillerud, K. P. A New Zirconium Inorganic Building Brick Forming Metal Organic Frameworks with Exceptional Stability.

(147) Marshall, R. J.; Forgan, R. S. Postsynthetic Modification of Zirconium Metal-Organic Frameworks: Postsynthetic Modification of Zirconium Metal-Organic Frameworks. *Eur. J. Inorg. Chem.* **2016**, *2016* (27), 4310–4331. https://doi.org/10.1002/ejic.201600394.

(148) Ling, S.; Slater, B. Dynamic Acidity in Defective UiO-66. *Chem. Sci.* **2016**, *7*, 4706-4712. https://doi.org/10.1039/C5SC04953A

(149) Yang, K.; Jiang, J. Computational Design of a Metal-Based Frustrated Lewis Pair on Defective UiO-66 for CO_2 Hydrogenation to Methanol. *J. Mater. Chem. A* **2020**, *8* (43), 22802–22815. https://doi.org/10.1039/D0TA07051C.

(150) Theuergarten, E.; Schlüns, D.; Grunenberg, J.; Daniliuc, C. G.; Jones, P. G.; Tamm, M. Intramolecular Heterolytic Dihydrogen Cleavage by a Bifunctional Frustrated Pyrazolylborane Lewis Pair. *Chem. Commun.* **2010**, *46* (45), 8561. https://doi.org/10.1039/c0cc03474f.

(151) Theuergarten, E.; Schlösser, J.; Schlüns, D.; Freytag, M.; Daniliuc, C. G.; Jones, P. G.; Tamm, M. Fixation of Carbon Dioxide and Related Small Molecules by a Bifunctional Frustrated Pyrazolylborane Lewis Pair. *Dalton Trans.* **2012**, *41* (30), 9101. https://doi.org/10.1039/c2dt30448a.

(152) Benseghir, Y.; Solé-Daura, A.; Cairnie, D. R.; Robinson, A. L.; Duguet, M.; Mialane, P.; Gairola, P.; Gomez-Mingot, M.; Fontecave, M.; Iovan, D.; Bonnett, B.; Morris, A. J.; Dolbecq, A.; Mellot-Draznieks, C. Unveiling the Mechanism of the Photocatalytic Reduction of CO_2 to Formate Promoted by Porphyrinic Zr-Based Metal–Organic Frameworks. *J. Mater. Chem. A* **2022**, *10* (35), 18103–18115. https://doi.org/10.1039/D2TA04164B.

(153) Faizan, M.; Pawar, R. Alanine Boronic Acid Functionalized UiO-66 MOF as a Nanoreactor for the Conversion of CO_2 into Formic Acid. *J. Comput. Chem.* **2023**, *44* (18), 1624–1633. https://doi.org/10.1002/jcc.27113.

(154) Mitoraj, M. P.; Michalak, A.; Ziegler, T. A Combined Charge and Energy Decomposition Scheme for Bond Analysis. *J. Chem. Theory Comput.* **2009**, *5* (4), 962–975. https://doi.org/10.1021/ct800503d.

(155) Cauwenbergh, R.; Goyal, V.; Maiti, R.; Natte, K.; Das, S. Challenges and Recent Advancements in the Transformation of CO_2 into Carboxylic Acids: Straightforward Assembly with Homogeneous 3d Metals. *Chem. Soc. Rev.* **2022**, *51* (22), 9371–9423. https://doi.org/10.1039/D1CS00921D.

(156) Ermolenko, M. S.; Guillou, S.; Janin, Y. L. Pyrazole-3/5-Carboxylic Acids from 3/5-Trifluoromethyl NH-Pyrazoles. *Tetrahedron* **2013**, *69* (1), 257–263. https://doi.org/10.1016/j.tet.2012.10.034.

(157) Tomás, R. A. F.; Bordado, J. C. M.; Gomes, J. F. P. *P* -Xylene Oxidation to Terephthalic Acid: A Literature Review Oriented toward Process Optimization and Development. *Chem. Rev.* **2013**, *113* (10), 7421–7469. https://doi.org/10.1021/cr300298j.

(158) Bukharkina, T. V.; Grechishkina, O. S.; Digurov, N. G.; Krukovskaya, N. V. Kinetic Model of Ethyl Benzene Oxidation Catalysed by Manganese Salts. *Org. Process Res. Dev.* **2003**, *7* (2), 148–154. https://doi.org/10.1021/op9900986.

(159) Mian, M. R.; Chen, H.; Cao, R.; Kirlikovali, K. O.; Snurr, R. Q.; Islamoglu, T.; Farha, O. K. Insights into Catalytic Hydrolysis of Organophosphonates at M–OH Sites of Azolate-Based Metal Organic Frameworks. *J. Am. Chem. Soc.* **2021**, *143* (26), 9893–9900. https://doi.org/10.1021/jacs.1c03901.

(160) De Koning, M. C.; Van Grol, M.; Breijaert, T. Degradation of Paraoxon and the Chemical Warfare Agents VX, Tabun, and Soman by the Metal–Organic Frameworks UiO-66-NH_2, MOF-808, NU-1000, and PCN-777. *Inorg. Chem.* **2017**, *56* (19), 11804–11809. https://doi.org/10.1021/acs.inorgchem.7b01809.

(161) Wasik, D. O.; Martín-Calvo, A.; Gutiérrez-Sevillano, J. J.; Dubbeldam, D.; Vlugt, T. J. H.; Calero, S. Enhancement of Formic Acid Production from Carbon Dioxide Hydrogenation Using Metal-Organic Frameworks: Monte Carlo Simulation Study. *Chem. Eng. J.* **2023**, *467*, 143432. https://doi.org/10.1016/j.cej.2023.143432.